

TALLINN UNIVERSITY OF TECHNOLOGY
DOCTORAL THESIS
16/2023

Design Optimization Methods of Additively Manufactured Switched Reluctance Motor

EKATERINA ANDRIUSHCHENKO



TALLINNA TEHNIKAÜLIKOOL
DOKTORITÖÖ
16/2023

Kihtlisandustehnoloogia abil toodetud samm-mootori optimeerimise meetodid

EKATERINA ANDRIUSHCHENKO



Contents

Contents.....	4
List of Publications	6
Author’s Contribution to the Publications	7
1 Introduction	8
1.1 The Motivation of the Study	8
1.2 The Objectives of the Study	8
1.3 The Novelty of the Study.....	9
2 State of the art of optimization and additive manufacturing of switched reluctance motor	11
2.1 Switched Reluctance Motor-Drive	11
2.1.1 Design and Control of Switched Reluctance Motors.....	11
2.1.2 Challenges of Switched Reluctance Motors Application.....	14
2.2 Optimization Environment.....	15
2.2.1 Optimization Models.....	15
2.2.2 Optimization Algorithms	24
2.2.3 Optimization Methods	25
2.2.4 Optimization Types and Model/Algorithm Selection.....	25
2.3 Additive Manufacturing of Switched Reluctance Motor.....	26
3 Optimization and Additive Manufacturing of Switched Reluctance Motor.....	28
3.1 Design of Switched Reluctance Motor	28
3.2 Proposed optimization method	31
3.2.1 Initial Design Optimization	32
3.2.2 Sensitivity Analysis	37
3.2.3 Topology optimization	45
4 Conclusion.....	49
5 Future studies	50
References	51
Acknowledgements.....	57
Abstract.....	58
Lühikokkuvõte.....	59
Appendix	61
Curriculum vitae.....	122
Elulookirjeldus.....	123

List of Publications

The list of author's publications, on the basis of which the thesis has been prepared:

- I **Andriushchenko E.**, Mohammadi M. H., Lowther D. A., Heidari H., Kallaste A. (2022). Topology optimization of a 3D-printed switched reluctance motor. 2022 International Conference on Electrical Machines (ICEM), Valencia, Spain, pp. 1976–1980, 2022.
- II **Andriushchenko E.**, Kallaste A., Mohammadi M. H., Lowther D. A., Heidari H. (2022). Sensitivity analysis for multi-objective optimization of switched reluctance motors. MDPI Machines 10(7), 559.
- III **Andriushchenko E.**, Kallaste A., Belahcen A., Vaimann T., Rassolkin A., Heidari H., Tiismus H. (2021). Optimization of a 3D-printed permanent magnet coupling using genetic algorithm and Taguchi method. MDPI Electronics 10(4), 494.
- IV **Andriushchenko E.**, Kaska J., Kallaste A., Belahcen A., Vaimann T., Rassolkin A. (2021). Design optimization of a permanent magnet clutch with Artap framework. Periodica Polytechnica Electrical Engineering and Computer Science, 65(2), pp. 106–112, 2021.
- V **Andriushchenko E.**, Kallaste A., Heidari H., Belahcen A., Vaimann T., Rassolkin A. (2020). Design optimization of permanent magnet clutch. 2020 International Conference on Electrical Machines (ICEM), pp. 436–440, 2020.

Author's Contribution to the Publications

Contribution to the papers in this thesis are:

- I **Ekaterina Andriushchenko**, as the main author, has carried out the topology optimization of the motor and analysed the results. The paper was written by her.
- II **Ekaterina Andriushchenko**, as the main author, has carried out the sensitivity analysis of the motor and discussed the results. The paper was written by her.
- III **Ekaterina Andriushchenko**, as the main author, has carried out the shape optimization of the permanent magnet clutch using genetic algorithm and Taguchi methods. Ekaterina analysed the results of the optimizations and compared two methods. The paper was written by her.
- IV **Ekaterina Andriushchenko**, as the main author, has carried out the shape optimization of the permanent magnet clutch in collaboration with Jan Kaska and analysed the results. The paper was written by her.
- V **Ekaterina Andriushchenko**, as the main author, has carried out the shape optimization of the permanent magnet clutch and analysed the results. The paper was written by her.

1 Introduction

To date, electrical machines (EMs) and drives have been incorporated into a vast number of industrial processes and applications. Electrical motors are the major users of electrical energy. They consume more than 50% of the global electrical power [1], [2]. Therefore, the efficiency of the electric motors is crucial for sustainable industry development. Optimization is one of the promising approaches to enhancing the efficiency of electric motors [3].

Often, motor optimization can lead to intricate design geometries which cannot be produced using conventional manufacturing techniques [4]. Additive manufacturing (AM) provides wider production possibilities for complex optimized designs and opens new ground for motor efficiency improvement [5].

In this work, the optimization of a Switched Reluctance Motor (SRM) is studied and a novel multi-level optimization methodology is proposed and implemented. Major elements of optimization are reviewed such as optimization models, optimization methods, and algorithms. In the meanwhile, key steps of the SRM design and optimization are presented. Lastly, additive manufacturing possibilities are explored and the initial and optimal designs of the motor are manufactured.

1.1 The Motivation of the Study

SRM has been invented nearly two centuries ago, but there has not been a motivation for its development, due to its low efficiency and loud noise production [6]. Thanks to the rapid growth of advanced power electronics and various control possibilities, the SRMs have now the opportunity to be implemented in the industry [7]. However, not all the problems can be solved by applying power electronic devices to the SRM drive. SR motors have a lot of potentials, yet they own design complications due to their salient nature [8]. Literature shows that optimization of SRMs can help to overcome the SRMs' design issues and considerably improve their performance. On another hand, AM is strong support of motor optimization. Due to the vast design opportunities that AM provides for motor manufacturing, optimization can be carried out at a more delicate level [9]. Hence, this thesis was motivated by the optimization of an additively manufactured SRM using sophisticated optimization techniques.

1.2 The Objectives of the Study

The objective of the study is to carry out SRM design and optimization to increase the average torque of the motor, reduce core material consumption, and decrease the torque ripples. This work starts with the review and assessment of the optimization environment elements such as models, methods, and algorithms to gain a deeper understanding of optimization principles. Prior to the optimization, this study designs an SRM utilizing the classic SRM design method. Then, a new multi-level optimization methodology is proposed based on a promising optimization method – topology optimization (TO). TO is known to impose a high burden on computational resources [10]. To reduce the computational complexity of TO, the design space is compacted using initial parameter optimization and sensitivity analysis of advanced optimization parameters. Thanks to implementing such an approach, the design space of the whole SRM can be minimized to a very essential and prompting area. High-performance improvement can be noticed after the SRM optimization. Additionally, this work makes

a deep overview of the AM and highlights the AM prospects for the optimization of EMs, in particular, SRMs. Lastly, initial and optimal designs of the SRM are produced employing AM techniques.

The objectives of the study can be summarised as follows:

- Increase the average torque, reduce the torque ripple, and decrease the core material consumption of an SRM using optimization techniques.
- Select an optimization environment suitable for additively manufactured SRM.
- Propose an optimization methodology with reduced computational complexity.
- Design an SRM taking into account AM possibilities.
- Acquire an optimal design of an SRM through the worked-out optimization methodology.
- Verifying results through modeling and prototyping using AM techniques.

1.3 The Novelty of the Study

One of the key elements of the motor optimization process is motor modelling. Motor modeling method plays an important role in defining the quality of the optimization results and time consumption [3]. In this thesis, SRM modeling methods are carefully studied and the classification of the methods is created. Based on the major characteristics such as accuracy, flexibility, rapidity, and simplicity, the SRM modeling methods are compared.

Through a wide literature review, major optimization models, methods, and algorithms of SRM optimization are defined and studied in detail. The importance of the correct selection of these key elements of the optimization can not be overlooked, since it plays the biggest role in the result of the optimization [11]. The models, methods, and algorithms are carefully compared in the scope of the SRM optimization.

In this thesis, the optimization approaches are scrutinized and assessed in detail. The TO approach is found to be promising and beneficial for SRM design, yet it yields extremely high computational costs [4], [12]. To overcome the issue of high computing effort, a novel optimization approach is designed. This approach considerably shrinks out the design space of the TO by carrying out two pre-optimizations: initial design optimization, and sensitivity analysis. The initial design optimization helps to optimize global design parameters such as the diameters of the rotor and stator, and teeth openings. Then, sensitivity analysis explores the influence of the shape of the rotor and stator on the motor performance and helps to define the most crucial areas. These vital areas of the motor geometry are then selected as search spaces of the TO. Thanks to this approach, the search space and, consequently, the time consumption of the TO can be reduced by more than 70%.

As a part of the optimization, sensitivity analysis provides valuable information about the influence of motor design parameters on the average torque and torque ripple of the SRM. This works presents the dependence of the torque characteristic on the tooth angle of the rotor and stator both at the air gap and at the core, eccentric air gap, and additional tooth implementation.

The outcomes of the SRM optimization are the initial optimal design, sensitivity analysis optimal design, and TO optimal design. These three designs not only present a

significant improvement of the SRM's torque characteristics but also contrast different optimization methods revealing their opportunities and challenges.

As a part of this thesis, the initial and optimal designs were produced using AM techniques.

The novelties of the study can be summarised as follows:

- SRM modelling methods are classified. Based on the major characteristics such as accuracy, flexibility, rapidity, and simplicity, the SRM modelling methods are compared.
- Various methods and algorithms are carefully compared in the scope of the SRM optimization.
- A novel optimization approach is designed. This approach considerably shrinks out the design space of the TO by carrying out two pre-optimizations: initial design optimization, and sensitivity analysis.
- As a part of the optimization, sensitivity analysis provides valuable information about the influence of motor design parameters on the average torque and torque ripple of the SRM.
- The outcomes of the SRM optimization are the initial optimal design, sensitivity analysis optimal design, and TO optimal design.
- As a part of this thesis, the initial and optimal designs were produced by means of AM techniques.

2 State of the art of optimization and additive manufacturing of switched reluctance motor

This section is based on the publications [11] where the optimization environment of the SRM is investigated. Besides, a detailed study of the design and control of the SRM drive is carried out and challenges of the SRM implementation are defined. A comprehensive comparison of the optimization modeling methods is presented, as well as the comparison of the optimization methods and algorithms in terms of accuracy, rapidity, flexibility, and simplicity.

2.1 Switched Reluctance Motor-Drive

2.1.1 Design and Control of Switched Reluctance Motors

Prior to the optimization of a motor, it is important to thoroughly understand the design, operation principle, and drive of the motor. Therefore, this chapter focuses on the essentials of the SRM design, working principles, and control.

Key highlights of the SRM design are its simple rigid structure, and lack of windings or permanent magnets on the rotor. As Figure 2-1 suggests, a three-phase SRM consists of a stator with six teeth that are carrying the windings, and a rotor that has four teeth and no magnets/windings.

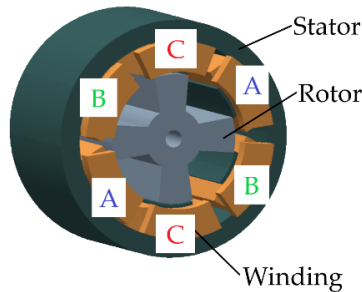


Figure 2-1: Structure of three-phase 4/6 pole SRM [8].

Depending on the position of the rotor, the inductance of an active phase is continuously altering. As can be seen in Figure 2-2 and Figure 2-3, the inductance is at its minimum, when the rotor and stator teeth are misaligned. At a certain position, when the corners of the stator and rotor teeth get close enough, the inductance starts increasing. During the period, when the inductance is growing, a constant torque can be produced. After the teeth of the rotor and stator fully align, the active phase inductance reaches its maximum and torque becomes zero. Near this position, another phase should get excited in order to produce the torque as in Figure 2-2.

The mathematical formulation of the described process of torque production is as follows:

$$T(\theta, i) = \int_0^i \frac{\partial L(\theta, i)}{\partial \theta} di. \quad 2.1$$

where T is the produced phase torque, θ denotes the rotor position angle, and i is the phase current.

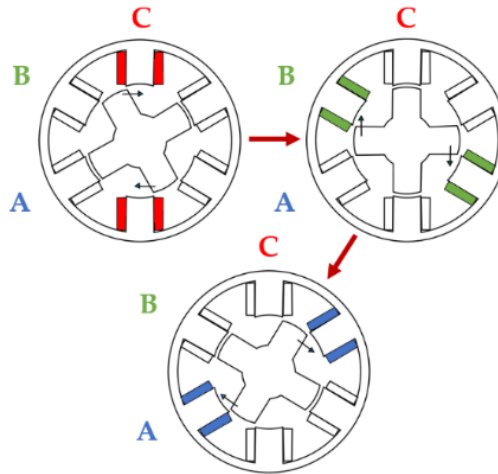


Figure 2-2: Rotation principle of SRM [8].

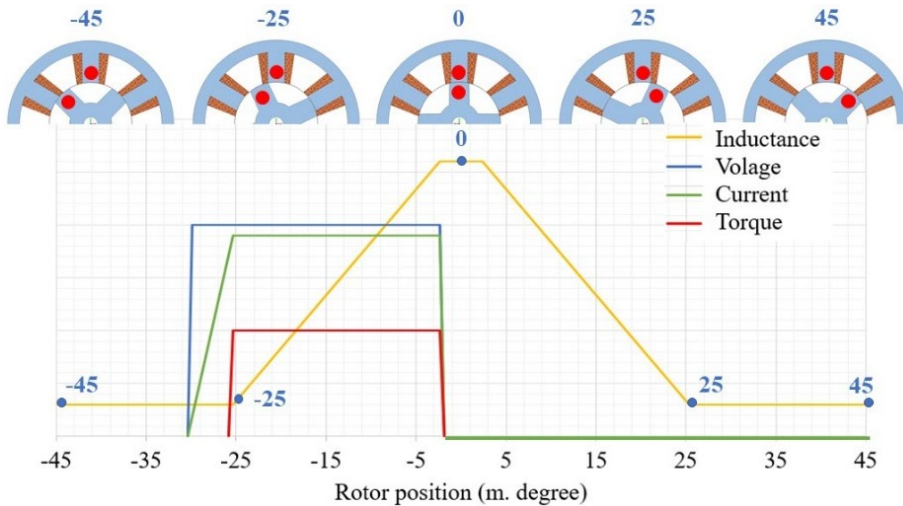
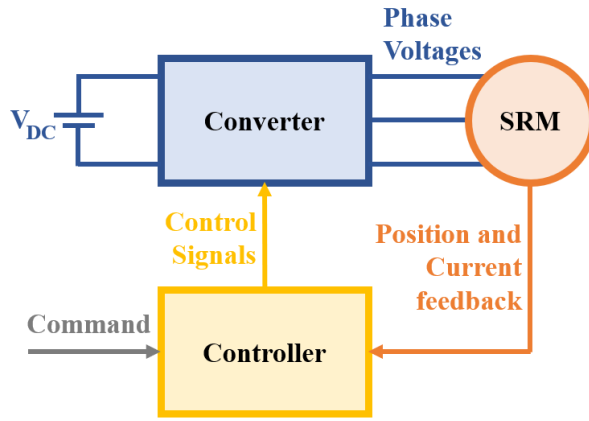


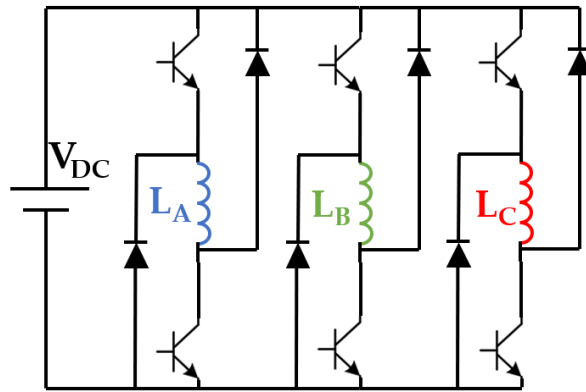
Figure 2-3: Ideal inductance profile of SRM's one phase [8].

A classic drive concept and control scheme of a three-phase SRM is presented in Figure 2-4. It can be seen from the Figure 2-4 (b) that each phase of the motor is controlled autonomously. The SRM control requires two switches per phase, which are controlled by the rotor position and current. The rotor position control is necessary in order to switch the driving phases at the right moments, and the current control is required to regulate the defined reference current value.

Frequently, the phase inductance profile of SRM defines the commutation pattern of the drive. For the three-phase SRM, the duration of the inductance growing phase is 30 mech. deg. Consequently, each of the phases should be turned on for 30 mech. deg with a step of 90 mech. deg. Yet, there are drive circuits that involve the overlapping of two phases with each other (see Figure 2-5).

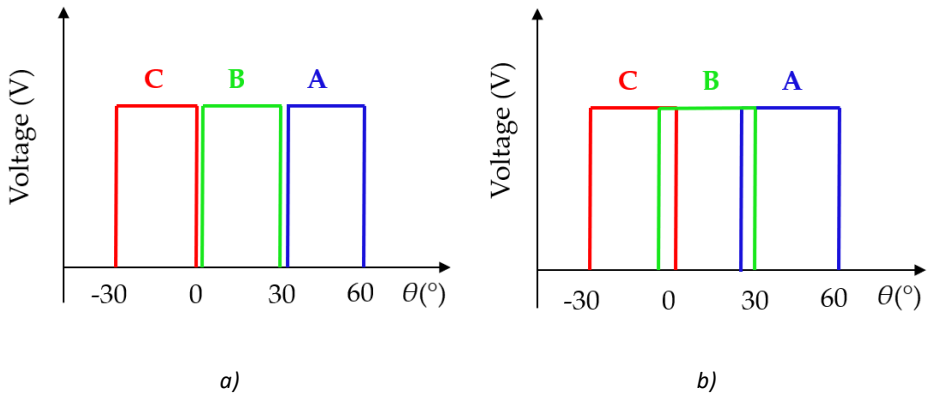


a)



b)

Figure 2-4: SRM drive: (a) SRM drive concept; (b) Asymmetric bridge converter [8].



a)

b)

Figure 2-5: Commutation pattern of three-phase SRM drive [8].

2.1.2 Challenges of Switched Reluctance Motors Application

A key challenge of the SRM application is closely related to the inductance profile of the motor phases. The inductance profile presented in the Chapter 2.1.1 is called the “ideal inductance profile”. It can be used for simplified estimation of the motor behavior. In reality, the inductance profile of the SRM is non-linear and called the “real inductance profile” (see Figure 2-6). Due to the salient nature of the SRM, its phase inductance is growing non-linearly due to the appearance of the fringing flux at the beginning of the rotor and stator teeth overlap (see Figure 2-7). The nonlinearity of the inductance leads to the nonlinear growth of the current and torque. Therefore, the SRM is characterized by high torque ripple and, thus, high vibration and noise levels while operating.

To overcome the issue of the torque ripple, the researchers have defined two solid approaches. One approach is related to the control of the motor. It has been shown, that the correct definition of the commutation parameters and currents can considerably improve the torque characteristics of SRMs. Another approach is focused on motor design and optimization. The literature presents many examples of torque improvement thanks to the introduction of certain teeth shapes of both stator and rotor.

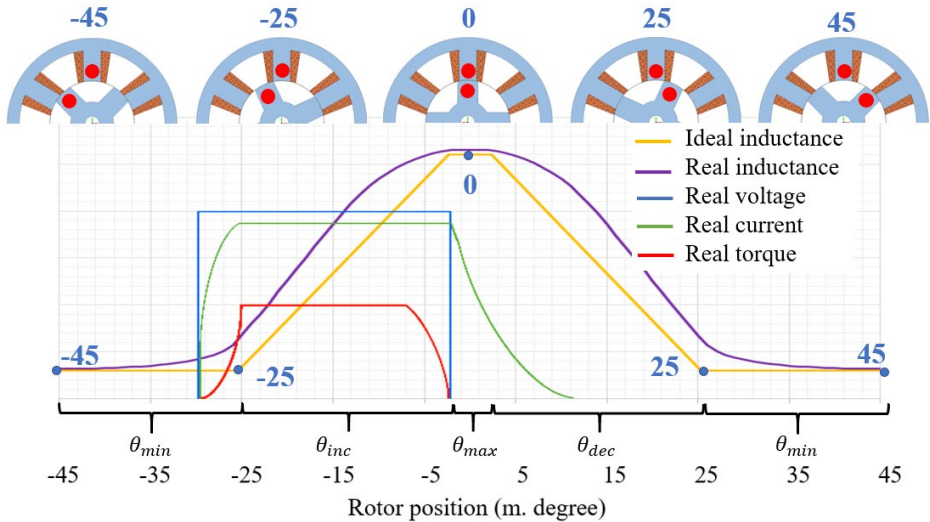


Figure 2-6: Ideal and real phase inductance comparison [8].

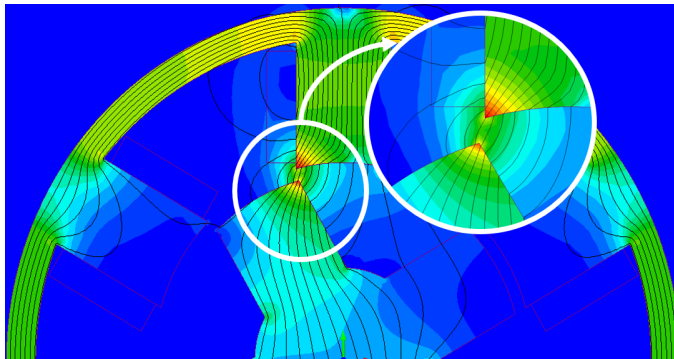


Figure 2-7: Fringing flux at the beginning of overlap [8].

2.2 Optimization Environment

Recent literature shows, that optimization is an effective tool that is used to improve the performance of EMs. For the EMs, optimization is a process of finding a set of design or control parameters that leads to the best (targeted) performance characteristics of the motor. The key elements of an optimization are the optimization model, optimization method, and optimization algorithm.

2.2.1 Optimization Models

An optimization model can be defined as a mathematical or numerical formulation of an optimization task. Usually, an optimization model includes:

1. The objective function, defines the aims of optimization such as maximization of average torque, maximization of torque density, minimization of torque ripple, minimization of mass, etc;
2. Constraints, define certain limits necessary for the optimal result such as iron losses less than 10 W, average torque more than 100 N, iron volume less than 10 l, etc. The objective function and constraints are sometimes interchangeable depending on their formulation and importance for the targeted designs;
3. Optimization parameters, which define the geometrical or control parameters of the motor. By varying the optimization parameters, an optimal set of them can be found that leads to the best-targeted performance of the motor.

The optimization model is responsible for forecasting the objectives and constraints for a particular set of optimization parameters. The optimization model can be defined as an analytical, numerical, or magnetic circuit (MEC) model. Basically, an optimization model is a design model which has the freedom to change design/control parameters in order to search for their optimal set.

In general, the design of an SRM involves several stages such as electromagnetic analysis, structural analysis, and thermal analysis. Usually, for each of these stages, a model should be created. In this thesis, only the electromagnetic basis of the optimization will be covered. Therefore, this section will be focused on the electromagnetic modeling of SRMs. Yet, some overview is given for thermal and structural analysis.

The main task of the electromagnetic modeling of an SRM is to find out the relation of the flux linkage ψ , phase voltage V , phase current i , and phase resistance R . Then, the key performance characteristics can be defined such as torque, losses, and efficiency.

$$\frac{d\psi}{dt} = V - Ri \quad 2.2$$

As it was mentioned in Chapter 2.1.2, the great challenge of the SRM design is the nonlinearity of the inductance of the SRM. Together with the operation under high saturation, these two specialties of SRMs bring a great challenge to the simulation of the motor.

This section gives a deep overview of the SRM modeling methods such as analytical methods, numerical methods, and the magnetic equivalent circuit (MEC) approach [13].

2.2.1.1 Magnetic circuit approach

The MEC method has been extensively used for modeling EMs owing to its simplicity and fast results prediction [14]–[21]. Yet, the accuracy of this method is quite low since it often can not take into account such processes as fringing flux or high saturation of SRMs (see Figure 2-8). The working principle of the MIC is illustrated in Figure 2-9. As can be seen from the figure, each core element of the SRM is represented by a gray rectangle or permeance. Then, each winding is illustrated as a circle. Lastly, the dashed line represents the airgap permeances [14]. Using the scheme presented in Figure 2-9, a system of equations is built and solved based on the circuit laws.

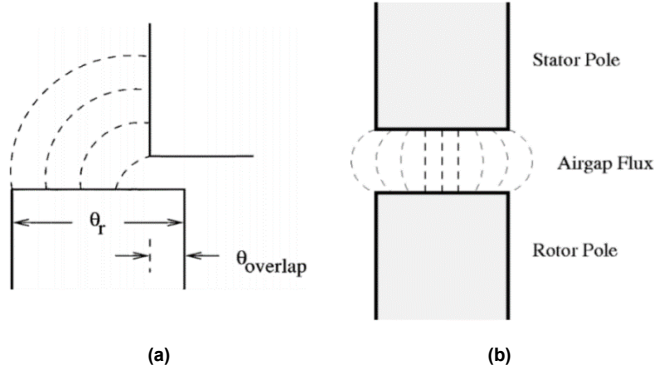


Figure 2-8: (a) Fringing effect in partial overlap position; (b) Fringing effect in complete overlap position [2].

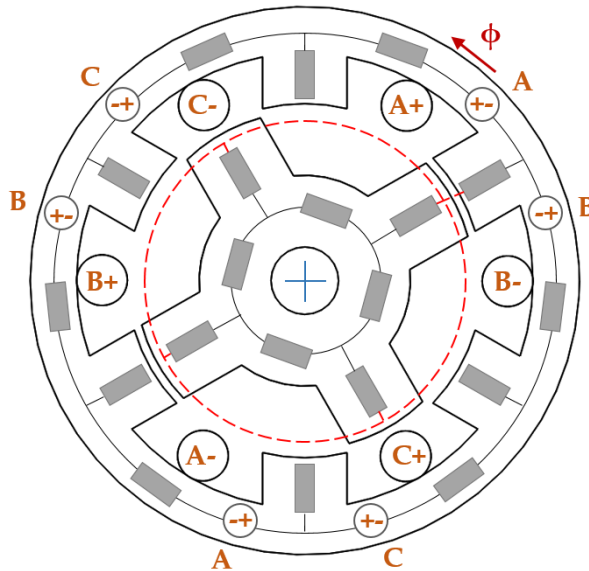


Figure 2-9: Magnetic circuit model of SRM [2].

To overcome the issue of lower accuracy, researchers attempted to take into account the high saturation of the rotor and stator pole tips by dividing the teeth into areas with different permeabilities [14]. Moreover, recent literature shows that the fringing effect

of the stator and rotor poles can be taken into account by appending the fringing air-gap permeance into MIC [19], [20]. For certain rotor positions, these MEC improvements lead to an accuracy comparable with the FE method while keeping the computation efforts low. Additionally, the MEC approach can be applied with the support of the FE method analysis [16]–[18]. The literature review showed, a 3D MEC method successfully combined with the FE-calculated fringing effect parameters [18]. This united technique has been validated by experimental results with high accuracy (see Figure 2-10).

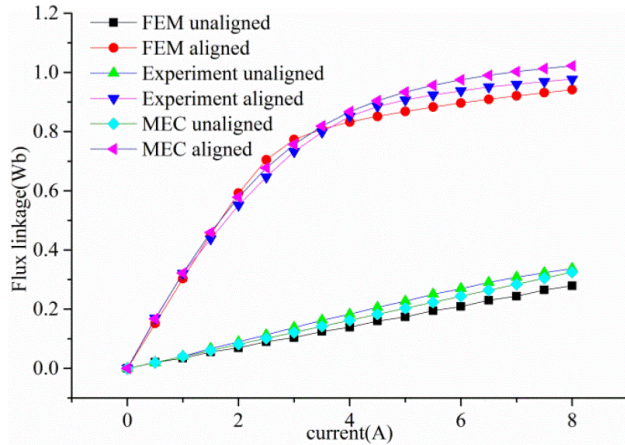


Figure 2-10: Comparison of flux linkage curves obtained by FEM, MEC, and experiment [6].

To the author’s knowledge, no literature presented the implementation of the MEC approach or MEC approach assistant by the FE method toward the optimization of SRM. A possible reason can be that there are limited possibilities to comprehensively parametrize the SRM within the MEC method. Basically, the freedom of the motor geometry modeled with MEC is relatively low, so the results of the optimization can hardly be significant.

2.2.1.2 Analytical approaches

For many years, analytical approaches have been broadly used for SRMs modeling. The analytical methods can be classified as follows:

- 1) Maxwell’s equation-based method
- 2) Interpolation methods
 - a) Lookup table-based interpolation method [22], [23]
 - b) Artificial neural network (ANN) based interpolation method [24]–[27]
 - c) Fourier-series-based interpolation method [28]–[31]

Maxwell’s equation-based method utilizes the magnetic potential \mathbf{A} together with Maxwell’s equations for solving 2D or 3D magnetic problems.

$$\nabla \times \mathbf{A} = \mathbf{B}, \nabla \cdot \mathbf{A} = 0 \quad 2.3$$

where \mathbf{B} is the magnetic field density. Together with Maxwell’s equation, equation 2.3 becomes:

$$\nabla^2 \mathbf{A} = -\mu \mathbf{J} \quad 2.4$$

where \mathbf{J} implies the current density and μ presents the magnetic permeability.

Maxwell’s method presents good accuracy and reliability, yet high computational complexity. Much research has been done on Maxwell’s method applied to SRM simulation [32]–[34].

To obtain the phase inductances of the SRM at arbitrary rotor positions, Sufei Li et al. devised a method employing Maxwell’s equation and conformal mapping technique. As it is shown in Figure 2-11, the proposed technique has a decent agreement with the FEA [33]. The alternative method offered in [34], simulates the magnetic field of the SRM operating under high saturation. The presented nonlinear analytical model has shown a positive correlation with FEM unlike the linear one (see Figure 2-12).

The MEC method, Maxwell’s equation-based approaches, and FEA require separate consideration of each operating condition of the machine. By contrast, the interpolation techniques propose models that can predict the performance of the machine based on a limited number of simulations or experimental tests. Therefore, a common feature of interpolation techniques is time efficiency.

A good example of an intuitive interpolation technique is presented in [23]. The authors utilized FEM analysis to construct a lookup table of the inductance characteristic depending on the rotor position and excitation. Using the lookup table along with a MEC, the dynamic characterization of the SRM was obtained. The benefit of this approach is that it is quite clear and smooth; however, its accuracy is not reasonable for some applications [29].

Nowadays, artificial neural networks (ANNs) based techniques are one of the most well-known tools for the interpolation of experimental or simulation data. ANNs have been extensively employed in numerous applications from forecasting and trends to signal processing and design optimization.

ANNs are essentially computing systems, which concept is inspired by the biological neural networks of human brains. Figure 2-13 illustrates the ANN working principle.

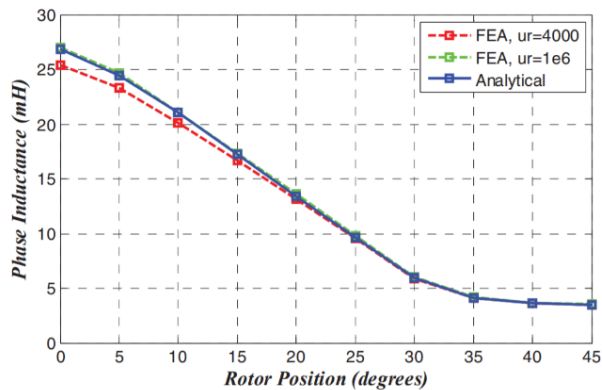


Figure 2-11: Comparison of the proposed analytical approach with FEA.

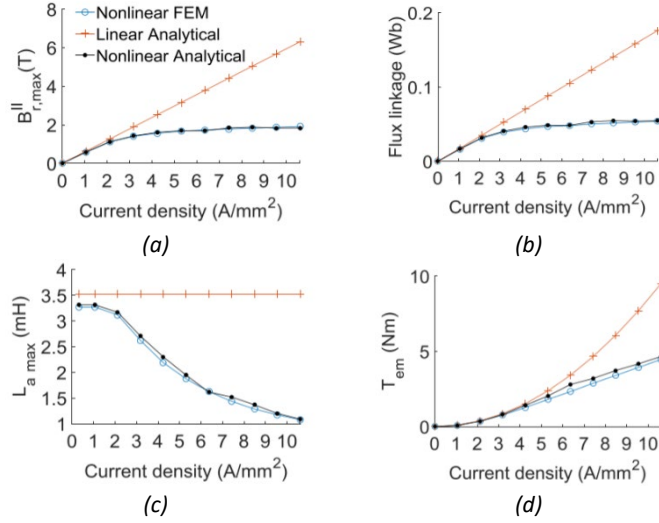


Figure 2-12: Performances versus current density with excitation in one phase. (a) Radial peak flux density values. (b) Flux linkage. (c) Maximum self-inductance. (d) Electromagnetic torque [22].

The neurons, which are the main components of a neural network (NN), accept inputs X_i , $i=1..n$. Then, the inputs together with the bias θ are multiplied by corresponding weight parameters. After that, the weighted inputs can be summed up to a set called net and then send to an activation function. Another way is to use a separate activation function for each weighted input and then, adding the bias, sum them up. The calculated result proceeds to the output. Additionally, Equation 3 illustrates the working principle of NN mathematically [35].

$$S = \sum_{i=1}^n w_i \cdot X_i + w_0 \cdot \theta,$$

$$\Omega_1 = f(S), \quad 2.5$$

$$\Omega_2 = \sum_{i=1}^n f_1(w_i \cdot X_i) + w_0 \cdot \theta,$$

where S introduces the set of the weighted inputs or net, while Ω demonstrates the set of outputs. Particularly, Ω_1 illustrates the case when the activation function is applied to the net S and Ω_2 illustrates the case when the activation function is applied to each weighted input.

Parameters of a NN such as weights and threshold of the inputs are defined through training a NN model. The activation functions are chosen by a user through experiments.

The ANN techniques have demonstrated several remarkable features, which are particularly useful in SRM design and simulation. For example, one of the unique qualities of ANNs is the ability to interpolate highly nonlinear systems. This quality is exceptionally valuable for modeling the nonlinear electromagnetic characteristics of the SRM. Moreover, previous research has demonstrated another advantage of the ANNs – the high accuracy of the interpolation models. On the other hand, the model's accuracy is greatly dependent on the training process and the provided training data.

An early example of the ANN application in the SRM design is presented in [26].

The research proposed a discrete-time model, which could simulate a faulty and fault-free SRM. The authors constructed a reliable ANN architecture with the support of the evolutionary algorithm (EA).

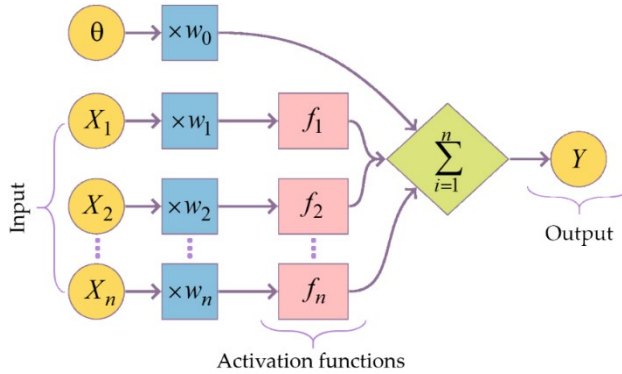


Figure 2-13: ANN working principle.

In a study conducted by W. Ding et al., the adaptive neural fuzzy inference system (ANFIS) techniques were used for modeling the SRM [36]. The researchers have been able to form an accurate and comprehensive SRM model verified by experimental data. Relatively recent research successfully utilized B-Spline NNs for online modeling of the SRM [37]. The online training of the B-Spline NN provided the obtained model with high robustness and accuracy.

To date, researchers have developed a list of effective methods based on the Fourier series for the SRM simulation. The following equation represents the considered Fourier series:

$$\lambda(i, \theta) = \sum_{k=0}^2 f_k(\theta) \cos(k\theta), \quad 2.6$$

where λ is the phase flux linkage, $f_k(\theta)$ are the series coefficients, i and θ are the phase current and the electric angle of the rotor, respectively.

Thanks to the possibility to change the number of Fourier terms used for interpolation, this approach proposes high flexibility of accuracy. Another advantage of this method is that the amount of data required for approximation is considerably lower than for the ANN interpolation method or FEM. Using a second-order Fourier series, S. Song et al. proposed a way to approximate the flux linkage of the SRM. Working just with 21 data points for determining the series coefficients, this method could demonstrate a good agreement with the test results (see Figure 2-14) [38]. A simple and reliable model of the SRM for real-time controller implementation was introduced in [30]. Additional consideration of the machine's geometry and materials makes this approach suitable within the design stage. Another good example of Fourier series usage for SRM modeling was presented in [39]. The researchers could successfully estimate the flux linkage profile without using complex and costly clamping devices and position sensors.

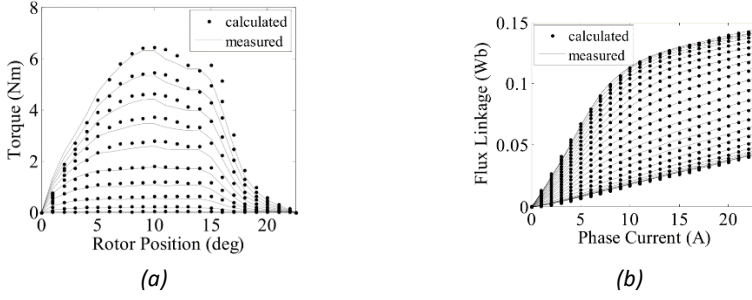


Figure 2-14: Calculated and measured SRM magnetic and torque characteristics [38].

There are not many papers, which show the implementation of the analytical methods within SRMs optimization. Yet, a new method called multiphase excitation used for the calculation of static torque taking into account the cross-coupling and magnetic saturation is introduced and utilized within the parameter optimization [40].

Another model widely utilized within the SRM optimization is a surrogate model. A surrogate model was initially developed for reducing the computational complexity of the optimization compared to FEM and obtain more precise results than through analytical methods. Basically, a surrogate model is a set of mathematical expressions which replace the FEM constructed using the design of experiment or ANN techniques. An example of the surrogate model utilization within the SRM optimization is presented in [41], where the flux linkage and torque characteristics are represented by the approximate models which are based on the data gained from the FEM.

2.2.1.3 Numerical Approaches

Simulating the SRM nonlinear behavior with good accuracy is a great challenge for researchers. Despite the merits of the MEC approach or analytical methods, the finite element method (FEM) is the most widely used way to model the SRM.

Principally, a FE model of an electromagnetic device is made up of finite elements, which carry the following information: geometry, materials, excitations, and constraints. A simple variation of the electric and/or magnetic potential exists within each finite element. Based on that, FE computing solves all the unknown electric and magnetic potentials and the associated fields. The classic formulation of the electromagnetic problem in FEA is A- ϕ (magnetic vector potential – electric scalar potential) formulation:

$$\begin{cases} \mathbf{B} = \nabla \times \mathbf{A} \\ \mathbf{E} = -\nabla\psi - \dot{\mathbf{A}}, \dot{\psi} = \varphi \end{cases} \quad 2.7$$

where B and E illustrate the magnetic and electric fields, respectively. Then, the final mathematical expression of a FE problem is the following:

$$[\mathbf{M}] \begin{Bmatrix} \dot{\mathbf{A}} \\ \dot{\psi} \end{Bmatrix} + [\mathbf{B}] \begin{Bmatrix} \mathbf{A} \\ \psi \end{Bmatrix} + [\mathbf{K}] = \{F_1(t)\} + \{F_2(t)\} \quad 2.8$$

where the A-partition of the equation illustrates Ampere's law, including induction and displacement currents, while the ψ -partition represents the charge continuity condition. Matrixes M, B, K are finite element matrices representing dielectric, conductivity, and reluctivity properties. The two load vectors F1 and F2 represent volume current loads and surface loads.

One of the primary benefits of the FEM is the ability to find an accurate solution for a

machine with complex, intricate geometry. Furthermore, this method can easily deal with anisotropic materials with nonlinear permeability. All these advantages make it particularly valuable in the SRM design.

There exists a considerable body of literature on the SRM simulation using the FEM [42]–[45]. To reduce the torque ripple of an SRM, an optimum rotor design has been found in [42] using the 2D FEM. Later, K. Kiyota et al. researched an SRM, where 2D and 3D-FEM analysis results were carefully compared with the tests (see Figure 2-15). It has been shown that the 3D-FEM analysis was capable of providing an accurate solution for an SRM design with an error of less than 5% [43].

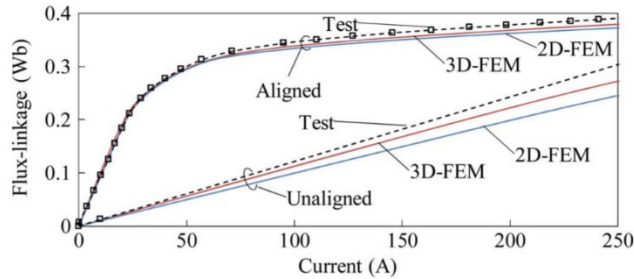


Figure 2-15: Flux linkage curve of the SRM [43].

Unfortunately, the 3D-FEM approach results in problems related to the model’s meshing. The mesh in a 3D-FEM model should have a high number of finite elements to achieve good accuracy. This makes up for the problem of high computational complexity and long execution time. This turns out to be even more problematic within an optimization, where thousands of machine designs should be analyzed. Certainly, the 2D-FEA can obtain simulation results much quicker compared to the 3D-FEA. However, the following limitations do not allow it to replace the comprehensive 3D-FEA:

- Alteration of material properties along the axial direction cannot be taken into account;
- Consideration of the machines with axial-field topologies is not possible;
- The flux linkage in the end-winding region is neglected;
- Eddy current losses related to steel lamination are not considered;
- Design features along the axial direction cannot be taken into account.

Despite the challenges of the FE implementation, many researchers have been intensively working toward 3D-FEA optimization. Several techniques have been proposed to improve the efficiency of 3D-FEA, some focusing on T- Ω (electric vector potential – magnetic scalar potential) problem formulation [46]–[48], others on the domain [49] or time decomposition [50]. These methods help to achieve a considerable reduction in the simulation time.

A huge amount of literature focuses on SRM optimization using FEA. For example, an SRM utilized in low-speed electric vehicles is multi-objectively optimized base on a FEM and the vehicle balance equations in [51]. In another paper, an SRM for high-volume traction applications is optimized by taking into account the control algorithm using FEA [52]. For SRM optimization, FEM proposes a great opportunity to create complex intricate geometries that is hardly possible using MEC or analytical techniques.

2.2.1.4 Modeling approaches comparison

To summarize the strengths and weaknesses of the modeling methods discussed in this section, Figure 2-16 is provided. In the figure, orange bubbles show the main groups of the electromagnetic design methods, and cyan bubbles illustrate a particular method. The methods are assessed in terms of accuracy, rapidity, flexibility, and simplicity. Each of these specifications has a particular color, which is assigned or not to a particular method. For instance, the highlighted attributes of the methods based on ANN are high accuracy and flexibility.

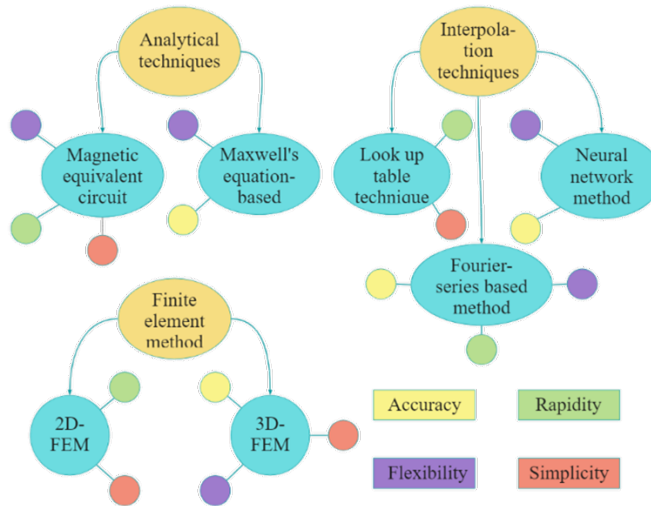


Figure 2-16: Comparison of electromagnetic analysis methods of SRM.

2.2.1.5 Structural and Thermal Analysis

Structural and thermal analysis are the important stages of motor development and optimization. Sometimes, due to the optimization, structural characteristics such as mechanical strength or manufacturability can be reduced. Therefore, for certain optimization problems, it is worth carrying out mechanical analysis after or during optimization. The key aspects of structural analysis are the following [53]:

- Mechanical stress/strain analysis
- Buckling analysis
- Vibration and noise analysis

Specifically, the mechanical stress/strain analysis is associated with a test of strength and aims to reveal whether the machine's structure and its components are able to bear the intended load without failure. By means of the buckling test, a designer ascertains that the machine and its components will not lose their stability. Finally, the vibration and noise analysis not only ensures that the machine's operation is stable but also guarantees that the noise produced by the machine is acceptable for the work environment.

Another key thing to remember within the structural analysis is an assessment of manufacturability. This process involves a determination of geometric dimensions and tolerances, setting up an appropriate fitness between mechanically mating parts of the machine.

It is known that one of the primary issues of SRM is the torque ripple and, consequently, the vibration and acoustic noise. The vibration and noise not only adversely affect the performance of the machine and its safety but also can be harmful to a human being. Moreover, the undesired vibration can easily damage the SRM parts such as stator windings, and rotor bearings, and even lead to failure. The vibration problem can be solved by approaching it through electromagnetic analysis and reducing the torque ripple. Additionally, the electromagnetic problem can be transferred to the mechanical analysis software and the vibration characteristics can be assessed directly [54]–[58].

Thermal analysis plays an important role in SRM design and optimization. The temperature of the machine strongly affects its performance, insulation life, mechanical strength, reliability, etc. Therefore, it is often important to check the thermal stability of a final optimization design or include the thermal characteristics in the optimization of SRM. The recent literature on EM design and analysis shows two major approaches used to carry out a thermal analysis. The first one is based on the equivalent heat circuit (EHC) [59], while the second employs numerical techniques such as computational fluid dynamics (CFD) and FEM [55], [60], [61], [62].

2.2.2 Optimization Algorithms

Using the optimization model, an optimization algorithm is aimed to find optimal designs, so-called sets of design parameters. An optimization algorithm is a set of mathematical operations which search for the best available alternative taking into account given constraints. So far, many optimization algorithms have been developed. Within the optimization of electrical machines, evolutionary algorithms, and particle swarm optimization algorithms appear to be the most prevalent.

The group of evolutionary algorithms (EAs) includes single- and multi-objective genetic algorithms, evolution programming, and evaluation strategy. All of these are inspired by biological evolution and use the knowledge of evolution's mechanisms such as reproduction, recombination, selection, and mutation. An overview of the EAs' terms and operations can be found in [63].

The evolutionary algorithms are widely applied in EM and electromagnetic device optimization. An example of an optimization of geometrical and control parameters of SRM using a non-sorting genetic algorithm II (NSGA-II) is presented in [52]. In another paper, the authors propose a new design optimization outline utilizing a fast-current profile estimation method and multi-objective differential evolution algorithm (DE).

As it is shown in the literature, the EAs have exceptional qualities. High algorithm flexibility, fast search space narrowing, and the capacity to find a global minimum are the main advantages to name. Yet, the optimization of the SRM using EAs can be computationally expensive.

The particle swarm optimization algorithm (PSO) is based on the birds' flock movement and was initially designed to simulate social behavior. This method defines a candidate solution and using a sequence of iterations tries to improve it. A comprehensive description of the algorithm theory and implementation can be found in [64]. There are many examples of PSO implementation for EM optimization. However, rarely it is used for SRM. One article presents a surrogate model coupled with the PSO algorithm for the multi-objective optimization of an SRM [64].

2.2.3 Optimization Methods

An optimization method is basically a procedure that solves the optimization problem using the optimization model and algorithm. There are three main groups of optimization methods used within the SRM design optimization: direct, indirect, and statistical optimization methods. The direct optimization method is a method that involves the direct interconnection of an analytical or FE model with an optimization algorithm. The indirect optimization method is one that uses a surrogate model for solving the optimization problem. And statistical optimization method involves a robust optimization model. As can be noticed, the key element that defines the optimization method is the optimization model.

2.2.4 Optimization Types and Model/Algorithm Selection

The selection of the modeling methodology and optimization algorithm strongly depends on the type of optimization and computational resources available. There are three types of SRM optimization:

- Parameter optimization [10]
- Shape optimization [63], [65]
- Topology optimization [10], [12]

Parameter optimization is an optimization where the geometry is controlled by linear and angular dimensions. Within the parameter optimization, the geometry always remains conventional. Therefore, the analytical modeling resources or FEA can be used for direct parameter optimization.

Shape optimization is an optimization where the geometry is controlled by surface lines, defining the shape of the motor. And topology optimization is an optimization where the geometry is defined by material distribution, sometimes, over the whole body of the motor. In the case of shape and topology optimizations, it is hardly possible to use analytical methods alone, due to the intricate shapes (or topologies) of the motor geometry. Moreover, there is no solid knowledge regarding the influence of various geometries of the motor on its performance. Therefore, the possible methods to be applied within the shape and topology optimization are the numerical method – FEM and partially numerical, partially analytical – surrogate modeling.

One of the promising but not yet widely applied optimization models within the SRM optimization is a robust optimization model. The key feature of a robust optimization model is that takes into account the manufacturing tolerances of a particular design and uses them while determining an optimal solution. In contrast with other optimization models where the aim is to define a global optimum, the robust optimization searches for a robust minimum which has a lower sensitivity to parameter variations. The optimization methods and algorithms associated with the robust optimization model are usually statistical and refer to the design of experiment (DoE) and Taguchi methods. An example of a robust optimization of an SRM is presented in [66], where the manufacturing tolerances are taken into account to ensure the robustness of the optimal solution.

Figure 2-17 compares the optimization models, methods, and algorithms discussed in this section.

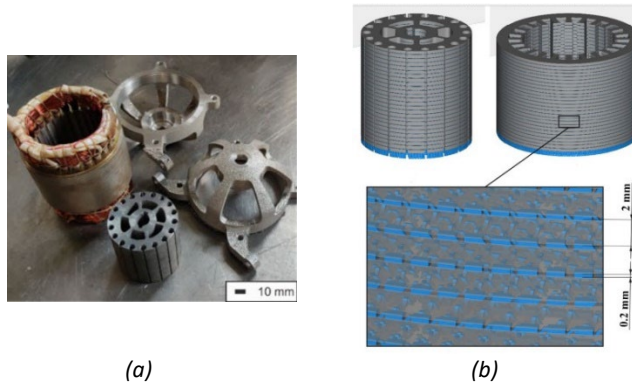


Figure 2-19: (a) 3D-printed IM; (b) rotor and stator core design [67].

Through the literature review, several challenges that AM development faces were revealed. It is well known that using conventional manufacturing techniques, the price of a single product decreases with the growth of the number of parts produced. In contrast with conventional manufacturing, AM does not allow the price of a part in mass production to decrease compared to a price of an individually produced part. In other words, an additively manufactured part will be the same expensive in mass production as in prototyping, because the amount of time and energy required to produce a part is the same [69]. Another challenge more related to EM basic characteristics is the eddy current which appears in a printed core of an EM. Due to the solid structure of the printed core and absence of laminations, EM experiences very high eddy current which can lead to poor performance and high core losses. Yet, there are promising possibilities of using lattice structures or lamination-like structures to reduce the eddy currents and achieve the performance presented by conventional EM as is presented in Figure 2-19 (b) [68], [70], [71]. Nowadays, AM has a limitation of using only one powder material for part production. Yet, for manufacturing automation and meeting the tolerances, it is necessary to use several materials how, for example, in coil manufacturing [72], [73].

Nevertheless, AM is a promising manufacturing possibility that is beneficial for the production of topologically optimized designs. Yet, the challenges presented in the previous paragraph should be addressed in the future.

3 Optimization and Additive Manufacturing of Switched Reluctance Motor

3.1 Design of Switched Reluctance Motor

Creating an initial design of an SRM has a quite well-established way. Usually, the key geometrical parameters such as bore diameter (D_r), and stuck length (L_c), have a direct relation to the output of the SRM.

$$T_e = K \cdot D_r^2 \cdot L_c \quad 3.1$$

where T_e is the output torque and K implies the output coefficient which is related to the electromagnetic loadings of the motor. The values of the output coefficient vary between 10 to 35 kN/m².

The next important step in creating the SRM design is to select the air gap length. Obviously, a smaller air gap in an SRM provides a higher inductance ratio and higher torque density. In this thesis, the air gap was set to the minimum possible to achieve according to the available tolerance limits of the manufacturing and was equal to 0.3 mm.

After defining the air gap, the stator inside diameter D_{si} and outside diameter D_{so} can be defined.

$$D_{si} = D_r + 2g, \quad D_{so} = (1.5 - 1.8)D_{si} \quad 3.2$$

where g is the air-gap length. The coefficient in front of D_{si} strongly depends on the number of stator poles. In this thesis, three phases 6 stator pole and 4 rotor pole SRM was considered. Therefore, a bigger coefficient was selected. Due to the size limitation of the 3D-printing machine to 80 mm, D_{so} was set to 80 mm. Other dimensions such as D_{si} , D_r were derived using equations (3.2) and were equal to 45 mm and 44.4 mm, respectively.

The stuck length of the motor is simply calculated using equation 3.3.

$$L_c = k \cdot D_r \quad 3.3$$

where k implies the length to bore coefficient and varies from 0.25 to 0.70 for non-servo and 1 to 3 for servo applications. In this thesis, the k was set to 1 and led to $L_c = 44.4$ mm.

Another important step of the SRM design is to define the configuration of the coil. Due to the decision not to use any cooling elements such as fans, etc., the current density was restricted to 5 A/mm². For a given current of $i=4$ A, the strand area of a wire was selected as 0.823 mm². The number of turns was selected such that the available winding space will be filled and was equal to 58 turns per coil.

Last but not least, the stator and rotor pole arcs are selected. Usually, to minimize the inductance at the unaligned rotor position, the total arc length of the rotor and stator poles should be shorter than the rotor pole pitch.

$$\beta_s + \beta_r < \frac{2\pi}{N_r} \quad 3.4$$

where N_r is the number of rotor poles. Classic stator and rotor pole values were used in this thesis and were equal to 30 mech deg.

The FE model of the described design was created using Simcenter MagNet software. The geometry of the initial design is illustrated in Figure 3-1. Additionally, the inductance profiles, static and transient torque are presented in Figure 3-2.

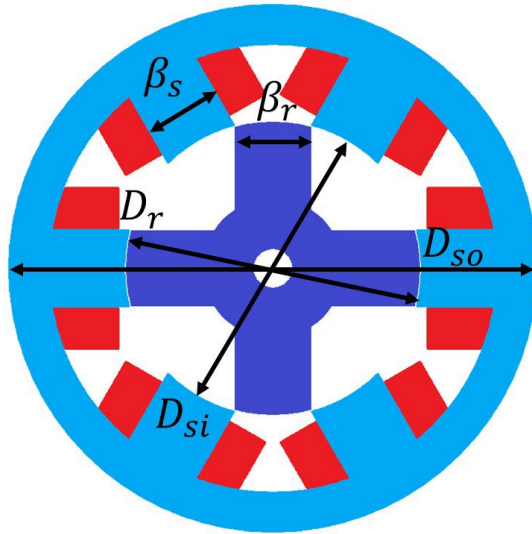
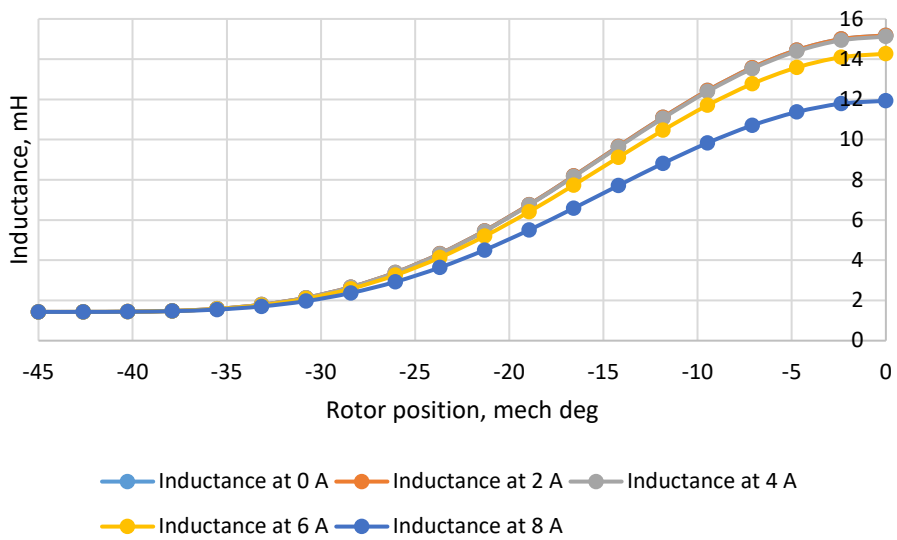
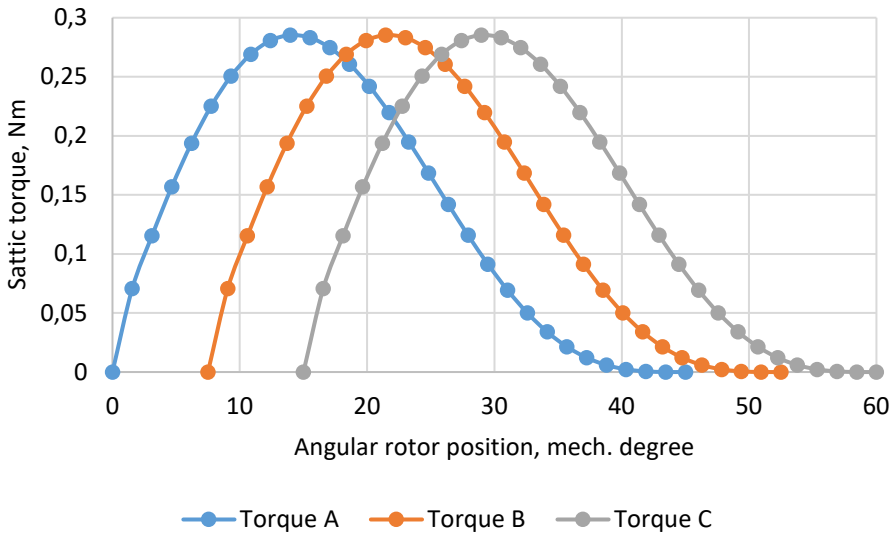


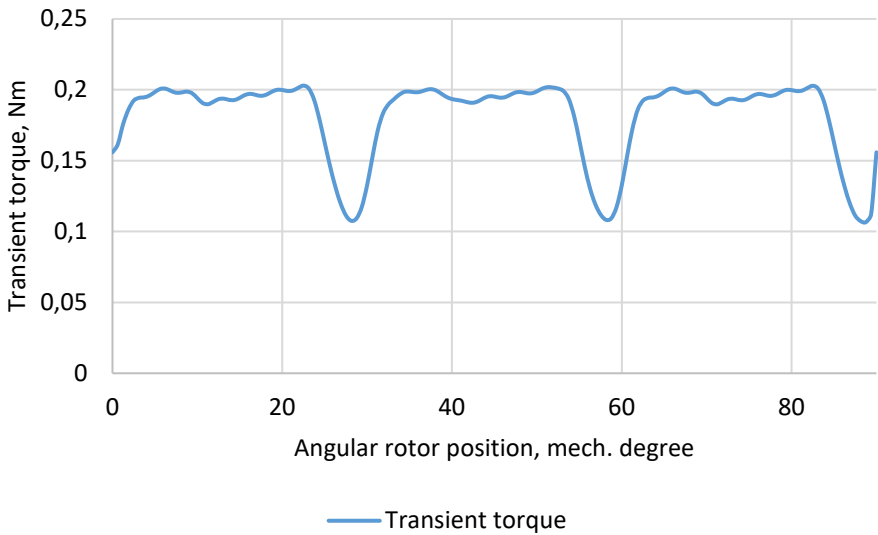
Figure 3-1: Initial design of SRM.



(a)



(b)



(c)

Figure 3-2: Initial design of SRM performance characteristics: (a) real inductance profiles, (b) static phase torques, and (c) transient torque.

3.2 Proposed optimization method

The TO is fast becoming a key instrument in EM optimization. Compared to the other optimization types such as parameter optimization and shape optimization, the TO proposes a vast variety of possible designs with the freedom to change not only the design parameters of SRM or motor shapes, but also the distribution of the material within a whole motor. The TO can play an especially important role in addressing the issue of SRM torque ripple, as geometrically very sensitive performance characteristics of SRM. As it will be shown in this section, design parameters, shapes, and material distribution within an SRM can significantly influence its performance.

In this thesis, turn-on/off topology optimization is considered. Essentially, the turn-on/off TO technique helps to optimize the layout of material in a given design space and includes the following steps: selection of design space, parametrization of the selected design space, and optimization.

The selection of design space for optimization is an important stage that has the biggest influence on the computational complexity and quality of optimization. The bigger the design space, the higher number of parameters needs to be used, consequently, the higher the computational burden is. It is essential to define the design space with optimal size and optimal location within a motor geometry. Depending on the objective of the optimization, the most influencing areas of an SRM need to be included in the design space. In this thesis, with the aim of reducing the computational complexity of TO, the design space was compacted using initial parameter optimization and sensitivity analysis of advanced optimization parameters. Thanks to implementing such an approach, the design space of the whole SRM can be shrinkaged to a very essential and prompting area of the SRM.

Parametrization of the design space essentially means that the design space is being divided into material cells, that can be filled in with material or with air. The number of parameters, their size, and shape can strongly influence the accuracy and the speed of the optimization. The parameterization of the considered SRM will be explained in detail in the following sections.

The optimization method is summarized in a flowchart (see Figure 3-3). Each of the milestones of the optimization is reflected in this flowchart and described in the following sections. Section 3.2.1 is dedicated to optimization model creation and initial optimization. Then, the sensitivity analysis procedure is described in Section 3.2.2 and the results are presented and discussed. Lastly, parametrization of the TO design space and TO optimization of the SRM is discussed in Section 3.2.3. Additionally, Section 3.2.4 summarizes key steps of the optimization integration using Matlab – MagNET software packages.

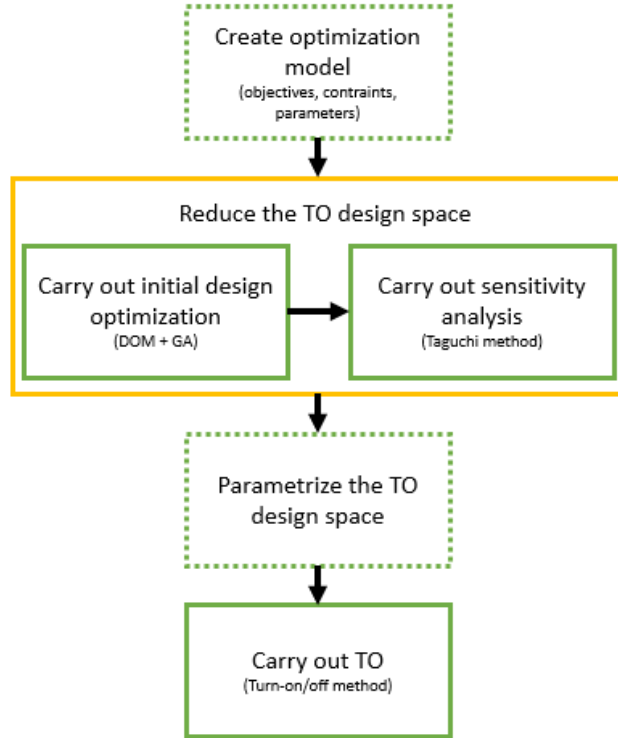


Figure 3-3: SRM optimization flowcharts.

3.2.1 Initial Design Optimization

As it is mentioned in earlier chapters, the main challenge of the SRM implementation is the torque ripples during the operation. It is well known that the reduction of the torque ripple often leads to the reduction of the average torque. Therefore, for the initial design optimization, it is worth finding an optimal design that can propose a good average torque while reducing the material volume of the core. Here, the reduction of the core volume directly affects the aim of the TO design space reduction.

3.2.1.1 Optimization model and method

The second step of the initial design optimization is to carry out the parametrization of the SRM. Six main geometrical parameters which are presented in Table 1 and Figure 3-4 were utilized for the optimization. Then, the optimization model can be mathematically formulated as follows.

$$\min f(D_{so}, D_{si}, D_{st}, D_{ri}, \beta_s, \beta_r) = [T_{peak}, V]^T \quad 3.5$$

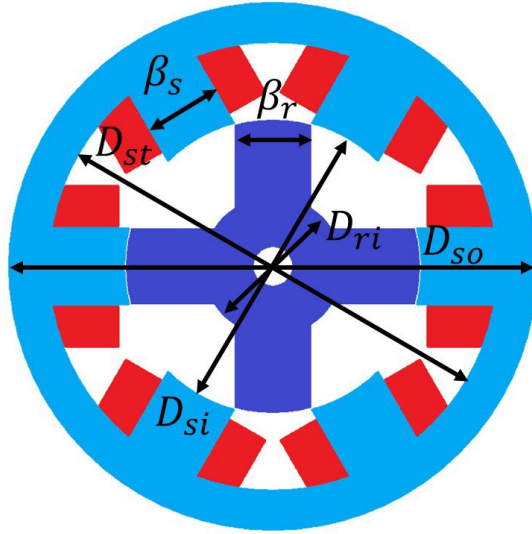


Figure 3-4: SRM initial optimization parametrization.

Table 3-1: SRM initial optimization parametrization

Parameter	Notation	Range
Stator outer diameter (mm)	D_{so}	70..80
Stator inner diameter (mm)	D_{si}	40..50
Stator teeth diameter (mm)	D_{st}	60..70
Rotor inner diameter (mm)	D_{ri}	10..15
Stator pole angle (°)	β_s	25..35
Rotor pole angle (°)	β_r	25..35

The initial design optimization was carried out using DOM, where a FE model of the SRM is optimized by an optimization algorithm. The flowchart of the initial design optimization is presented in Figure 3-5. In this thesis non-dominated Sorting Genetic Algorithm - II (NSGA-II) was applied within Matlab software package. To evaluate the torque of the SRM, a 2D FE adaptive model was constructed in Simscenter MagNET software [74]. More details on creating an adaptive parametrized model within Matlab – MagNET environment are presented in Section 3.2.4. Additionally, the windings of the motor were simulated in 3D, and additional resistance and inductance due to the end-windings were added into the 2D model. With the aim to reduce the computational complexity only one phase of the motor was simulated (see Figure 3-6). Furthermore, to achieve precise analysis results, the material of the core was created within MagNET software with the additively manufactured silicon steel characteristics presented in Figure 3-7.

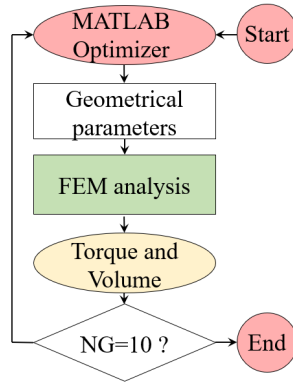


Figure 3-5: Initial optimization flowchart.

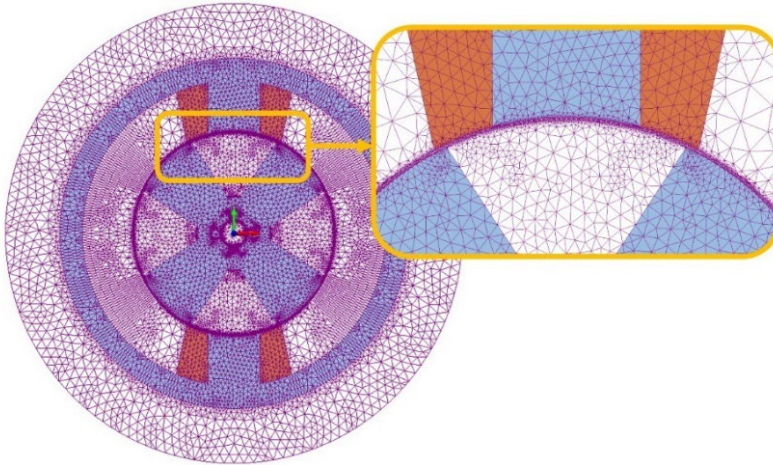


Figure3-6: SRM's 2D FE model for one phase [8].

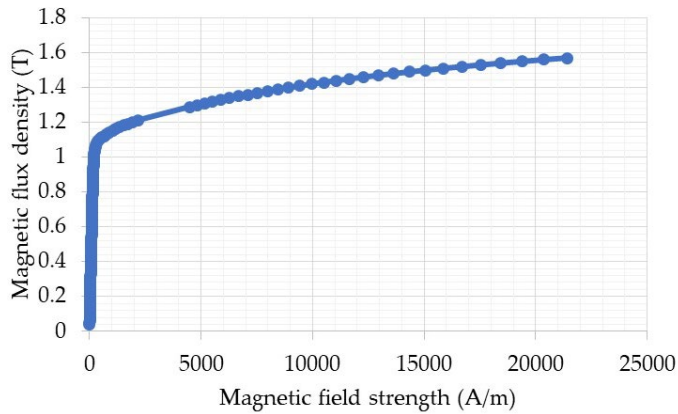


Figure 3-7: B-H curve of printed steel [63], [75].

3.2.1.2 Optimization algorithm

Lately, NSGA-II has been widely utilized for EM optimization due to its unique features such as the ability to find a global minimum of an optimization problem, handle problems in non-analytical form, and high flexibility. NSGA belongs to the group of evolutionary algorithms (EA) and multi-objective GA (MOGA) which defines its functional basis. Basically, NSGA-II is a method of solving constrained and non-constrained optimization problems using the principles of natural selection in biological evolution. A detailed explanation of the MOGA working principle is presented in [63].

The flexibility of NSGA-II is defined by the possibility of easily controlling the following parameters:

- Population size
- Number of generations
- Settings of the selection operator
- Settings of the crossover operator
- Settings of the mutation operator
- Stop criteria

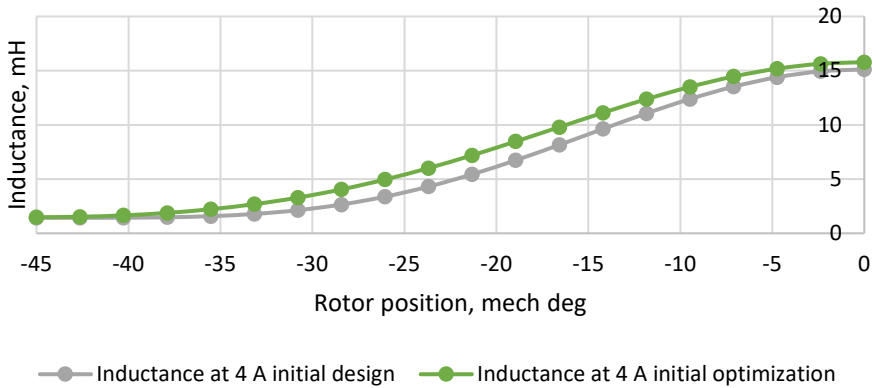
In this thesis, the optimization was carried out with 10 generations and a population size 100. The stop criteria were set as the competence of all 10 generations.

3.2.1.3 Optimization Results

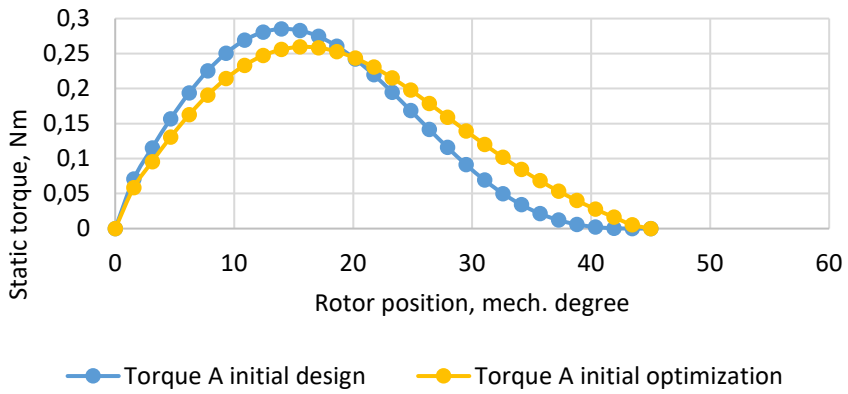
The optimization was successfully carried out within MagNET – Matlab environment. The comparison of the initial and optimal design is presented in Table 3-2 in numbers and in Figures 3-8 in the graphs listing the main performance characteristics of SRM such as inductance, static, and transient torque.

Table 3-2: SRM initial and optimal design dimensions

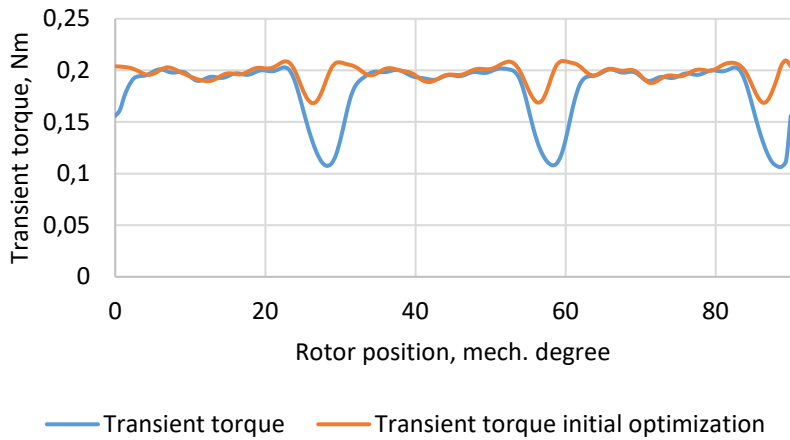
Parameter	Notation	Initial	Optimal
Stator outer diameter (mm)	D_{so}	80	80
Stator inner diameter (mm)	D_{si}	45	46.6
Stator teeth diameter (mm)	D_{st}	68	69.6
Rotor inner diameter (mm)	D_{ri}	21.2	17.1
Stator pole angle (°)	β_s	30	28.5
Rotor pole angle (°)	β_r	30	35
Volume (mm ³)	V	136575	137384



(a)



(b)



(c)

Figure 3-3: Comparison of the initial and optimal designs of SRM in terms of: (a) real inductance profiles, (b) static phase torques, and (c) transient torque.

What stands out from the presented figures is that the static torque improved its average value after the optimization: the initial average static torque was 0.13 Nm while the optimal was 0.14 Nm. Transient torque saw a considerable improvement as well: the initial average transient torque was equal to 0.181 Nm while the optimal was equal to 0.197 Nm. Moreover, with the new design, the torque ripple was significantly reduced from 0.53 to 0.21. Volume reduction was not noticed in the results due to the initially compact design of the motor. Yet, although the increase of the rotor pole angle was considerable, the optimization algorithm could keep the volume literally constant. The increase in average torque led to a 10% increase in the torque density from 1318 N/m³ to 1456 N/m³. The optimal geometry of the motor is presented in Figure 3-4.

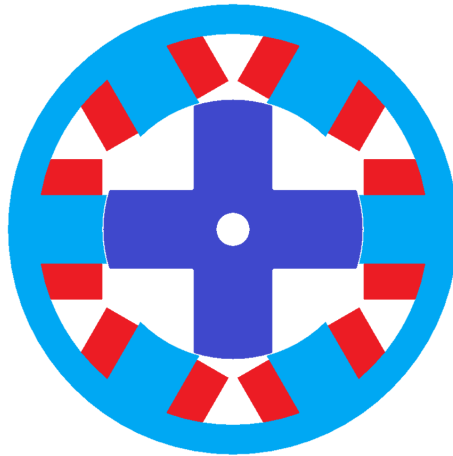


Figure 3-4: Initial optimal design of SRM.

3.2.2 Sensitivity Analysis

The aim of the sensitivity analysis in this thesis is mainly to reduce the computational complexity of the future TO by identifying the most crucial areas and parameters of the SRM design for torque ripple reduction and average torque increase. Taguchi's design of experiment (DoE) was used to carry out the sensitivity analysis due to its simplicity, rapidness, and reliability. A detailed description of the Taguchi DoE method is presented in [63].

3.2.2.1 Sensitivity analysis model and method

Through the extended literature review, a list of geometrical parameters was created for in-depth analysis of the SRM geometry. Figure 3-5 presents the parameters considered in this thesis: rotor pole angle, rotor pole angle at the core, stator pole angle, stator pole angle at the core, airgap shift, and additional tooth angle on the rotor. Rotor and stator pole angles are known to expressively affect the performance of SRM due to their direct influence on the inductance profile and duration of the minimum, maximum inductance, and duration of the growing and decreasing phases. On the other hand, angles at the core of both the stator and rotor were noticed in the torque ripple minimization. At the same time, an additional tooth angle at the core can propose a solution similar to the angles at the rotor and stator core. Last but not least, the airgap shift has shown an enormous influence on the torque ripple reduction. An in-depth description of the mentioned geometrical parameters is presented in [8].

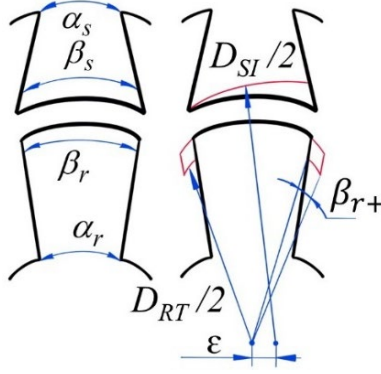


Figure 3-5: Sensitivity analysis parameters [8].

In this thesis, the parameters with the following constraints we assessed:

$$\mathcal{F}_{\Delta} = \begin{cases} 25^{\circ} \leq \beta_s \leq 40^{\circ} \\ \beta_s - 5^{\circ} \leq \alpha_s \leq \beta_s - 15^{\circ} \\ 25^{\circ} \leq \beta_r \leq 40^{\circ} \\ \beta_r + 25^{\circ} \leq \alpha_r \leq \beta_r + 50^{\circ} \\ 0 \text{ mm} \leq \varepsilon \leq 1 \text{ mm} \\ 0^{\circ} \leq 2 \cdot \beta_{r+} \leq 15^{\circ} \end{cases} \quad 3.6$$

Using the Taguchi method, the orthogonal array with the minimum necessary parameters combinations was constructed and consisted only of 25 designs. Thanks to the Taguchi method, the number of designs exploring six parameters with five levels each (see Table 3-3) could be considerably minimized compared to the full factorial experiment that would include more than 7000 designs.

Table 3-3: Design parameters' sampling.

Design Parameter / Control Factor	Symbol	Factor	Level				
			1	2	3	4	5
Stator pole angle (°)	$\beta_s = X_1$	X_1	25	28.75	32.5	36.25	40
Stator pole angle at core (°)	$\alpha_s = \beta_s - X_2$	X_2	5	7.50	10	12.50	15
Rotor pole angle (°)	$\beta_r = X_3$	X_3	25	28.75	32.5	36.25	40
Rotor pole angle at core (°)	$\alpha_r = \beta_r + X_4$	X_4	25	31.25	37.5	43.75	50
Airgap shift	$\varepsilon = X_5$	X_5	0	0.25	0.50	0.75	1
Additional tooth angle (°)	$\beta_{r+} = X_6/2$	X_6	0	3.75	7.50	11.25	15

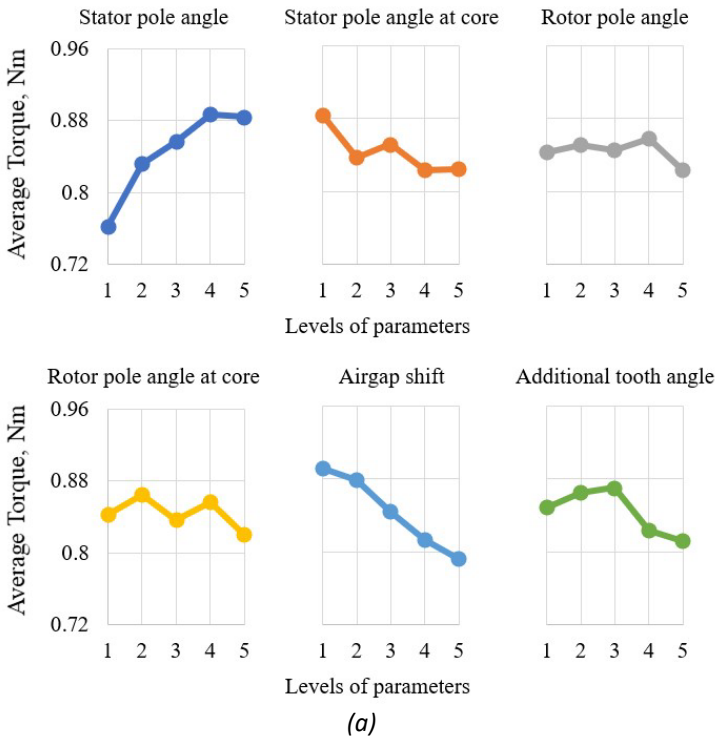
After all the designs were calculated and the objectives (the average torque, torque ripple) were assessed, their peak-to-peak values and a sum of squares were estimated for each parameter and level.

3.2.2.2 Sensitivity analysis results

The results of the sensitivity analysis are shown in Figure 3-6. It is worth mentioning, that these results should be considered as an example, illustrating the influence of various parameters on the torque characteristics. The presented figures were built for an SRM with slightly different dimensions, presented in [8].

According to the presented graphs, stator pole angle and air gap shift have the key influence on the average torque value. With the increase of stator pole angle, the average torque increases, while with the increase of the air gap, the average torque decreases. On the other hand, the enhancement of the air gap shift significantly reduces the torque ripple, while an increase in the rotor pole angle and the introduction of the additional tooth angle increases the torque ripple. The influences of the airgap shift and stator pole angle can be confirmed by the literature [76]. However, the negative influence of the rotor pole angle needed to be reassessed.

Figure 3-7 presents the results of the cross-check analysis of the transient torque for different rotor pole angles with the rest geometry of the motor fixed. It can be clearly seen that with the increase of the rotor pole angle, the average torque slightly increases. At the same time, the torque ripple gets impressively reduced until the rotor pole angle reaches 40°. The values of the average torque and torque ripple can be seen in Table 3-4. One of the reasons for the opposite result in Figure 3-6 (b) can be that the initial assessment was made with the static torque.



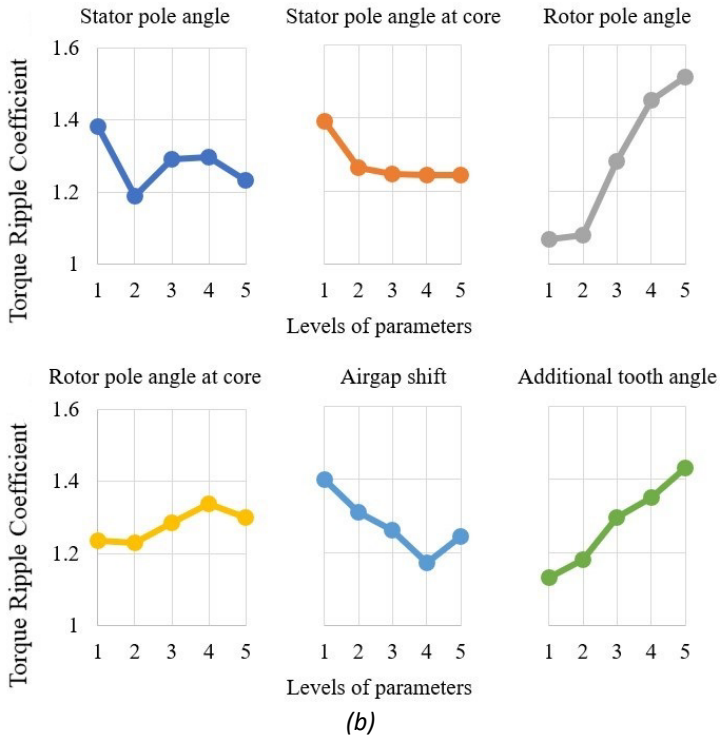


Figure 3-6: Peak-to-peak values of (a) average torque; (b) torque ripple [8].

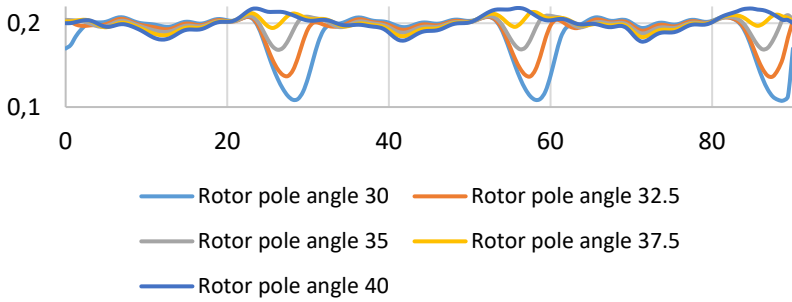


Figure 3-7: Rotor pole angle variation results.

Table 3-5: Rotor pole angle variation results.

Characteristic	Angle				
	30	32.5	35	37.5	40
Average torque, Nm	0.186	0.192	0.197	0.199	0.200
Torque ripple	0.537	0.371	0.210	0.148	0.199

Due to the high influence of the airgap shift on both average torque and torque ripple, it was highly beneficial to explore its influence in more detail. Within another case study, additional designs were explored, which can be defined by Figure 3-7 and Table 3-6. Figure 3-7 presents a slightly different but analogous definition of the air gap through the stator inner diameter shift and Table 3-6 maps this shift. Figure 3-8 presents interesting results obtained from this experiment. Using the airgap shift, the shape of the static torque can be visibly controlled. For instance, with the increase of the airgap shift, the torque becomes wider which is exactly helpful for the reduction of the torque ripple. At the same time, an increase in the airgap shift makes the torque reduce at the beginning and increase at the end of the torque production cycle. This way, torque can be forced to be more constant using an appropriate airgap shift. On the other hand, the average torque is obviously reducing with the increase of the airgap shift, which was also shown by the Taguchi sensitivity analysis.

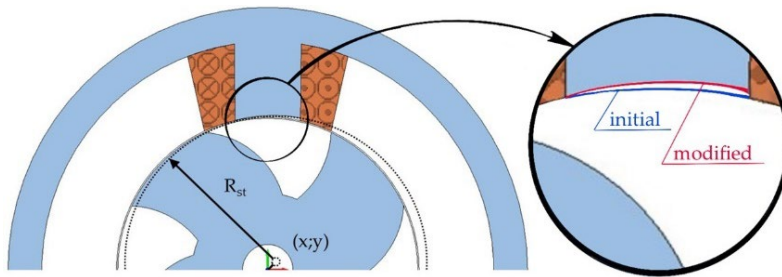


Figure 3-7: Schematic illustration of the second group of design modifications of the SRM.

Table 3-6: Design modifications parameters.

Design	Coordinates (x; y), mm
1st design modification	1; 0.30
2nd design modification	0.50; 0.15
3rd design modification	0.25; 0.07
4th design modification	0.125; 0.035

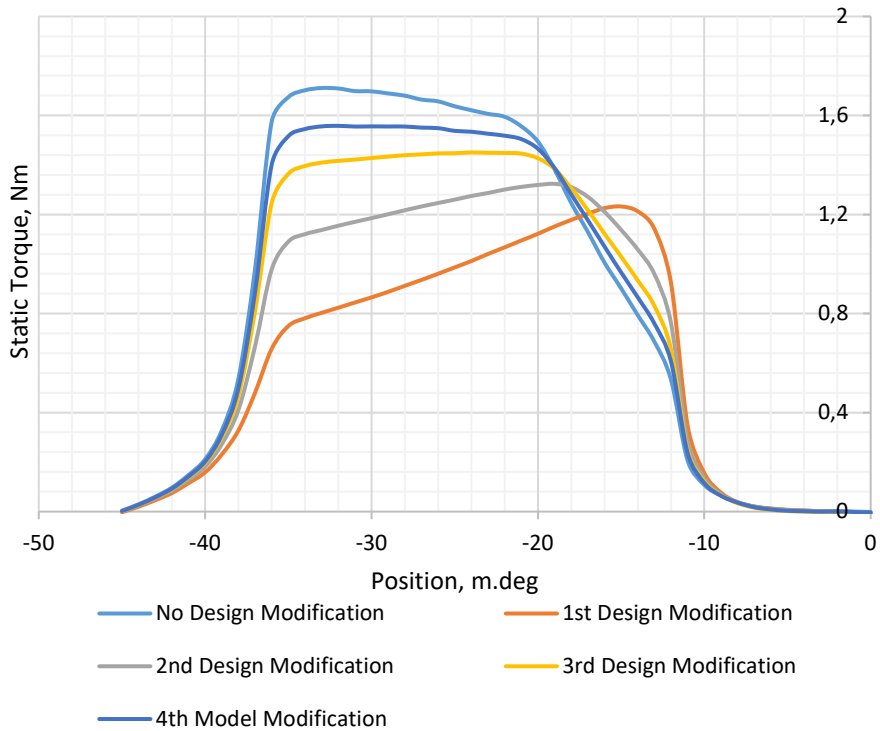


Figure 3-8: Airgap shift variation of the SRM.

The results of the sensitivity analyses indicated the most influencing areas of the SRM design. It was revealed that airgap shift variation, rotor and stator pole angles, and additional tooth angle of the rotor have a major impact on the average torque and torque ripple. To reduce the computational complexity, the following areas of the SRM were considered within the following TO (see Figure 3-9). Moreover, to speed up the calculations and future preparation of the prototype, only the rotor was topologically optimized in this thesis. Additionally, through the sensitivity analysis, an update of the rotor geometrical parameters was done with the aim to reduce the torque ripple and increase the average torque. A comparison of the initial design, initially optimized design, and design selected by the SA is presented in Figure 3-10. As can be noticed, transient torque shows a slight increase in the average torque to 0.199 N/m and a reduction of the torque ripple to 0.152. Moreover, Figure 3-9 shows not only the area of interest for future TO but also reflects the geometry of the new design. It is important to notice, that the results of the sensitivity analysis such as updates in the geometry and selection of the crucial areas for the TO, lead to a more than 70% decrease of the future TO design space.

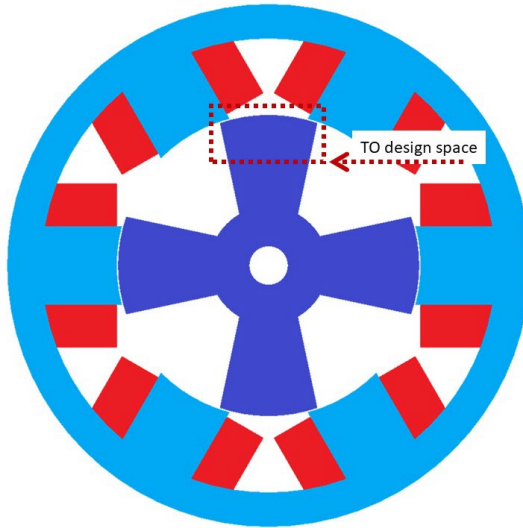
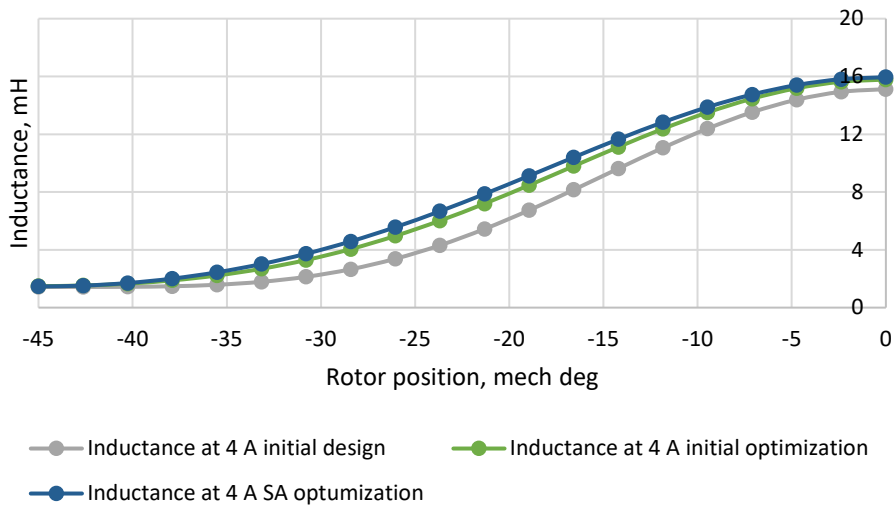
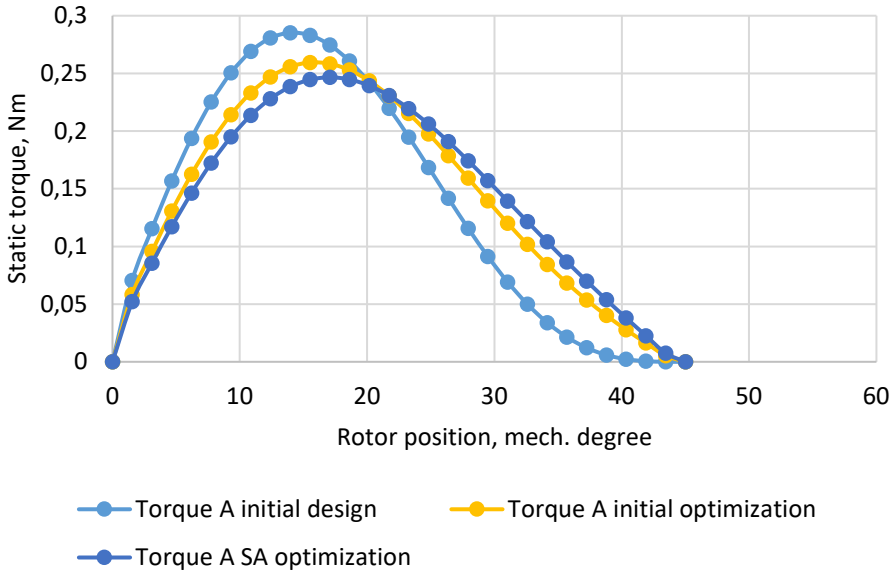


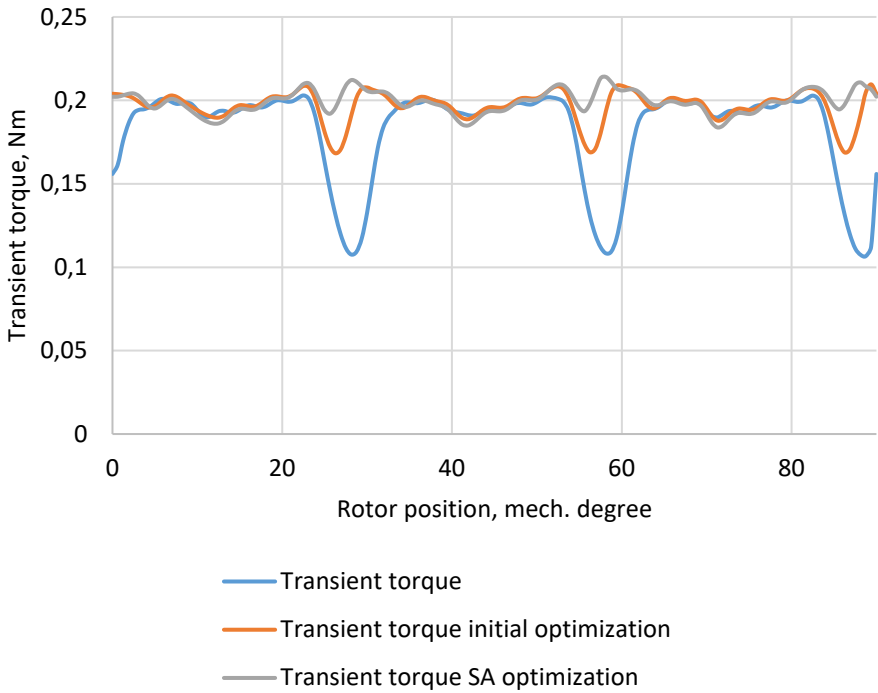
Figure 3-9: TO design space with SA optimal design.



(a)



(b)



(c)

Figure 3-10: Comparison of the initial, initial optimal, and SA optimal designs of SRM in terms of: (a) real inductance profiles, (b) static phase torques, and (c) transient torque.

3.2.3 Topology optimization

TO is known to be a powerful tool used for motor optimization. Very well established in mechanical design, the TO method starts opening new ground in electromagnetics as well [77]. Several studies have shown that TO can considerably reduce the torque ripple in reluctance motors [12], [78].

Several types of TO exist, one of the most widely applied is the On/Off TO method. As it was mentioned before, the On/Off optimization method uses the material distribution over the design space as optimization parameters. The design space parametrization which was applied within this thesis is presented in Figure 3-11. As can be seen, the design space is divided into many sections, in our case 150, which are considered optimization parameters. To reduce the number of parameters and prevent a chess board-like structure, parameters were grouped between each other in shapes “L” or rotated “L”. This way, only 50 parameters were participating in the TO.

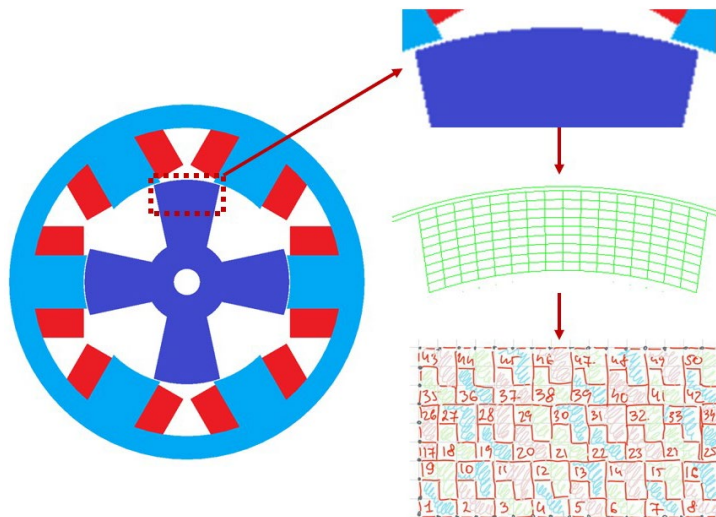


Figure 3-11: TO design space parametrization.

A single-objective optimization was performed with the aim to minimize the torque ripple. Due to the restrictions of the optimization algorithm of Matlab software associated with the TO discrete nature of the parameters, only one objective could be targeted. As in the initial optimization, NSGA-II was utilized along with a transient model of the SRM.

The resulting geometry is presented in Figure 3-12 as well as the main electromagnetic characteristics are shown in Figure 3-13. As can be seen on the transient curve graph, the average torque slightly increased to 0.201 N/m, while the torque ripple decreased to 0.123. The inductance curve and static torque did not experience many changes. The obtained shape has formed two distinguishing islands. Gained asymmetry of the rotor teeth can be described by the clock-overwise rotation of the rotor during the simulation.

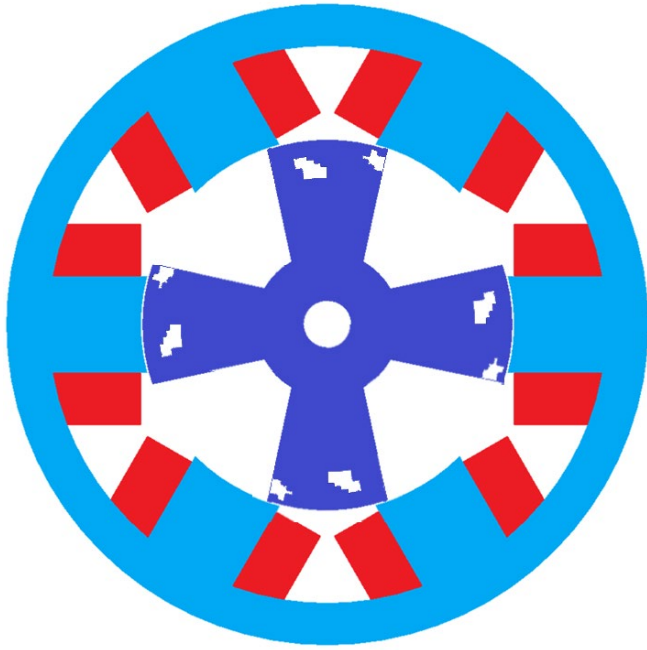
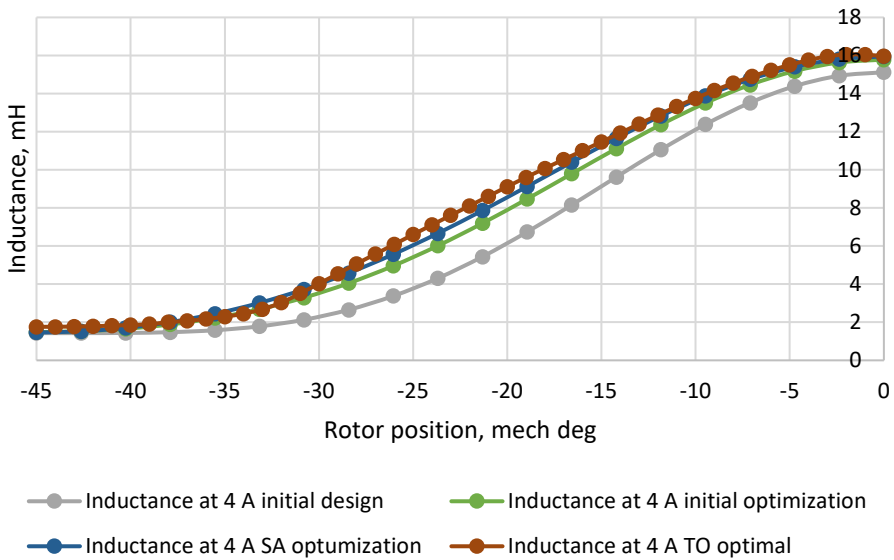
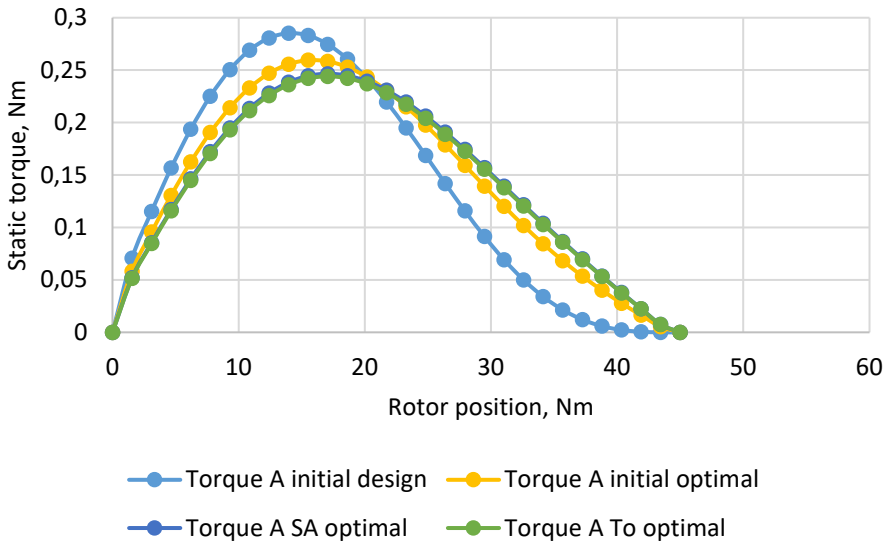


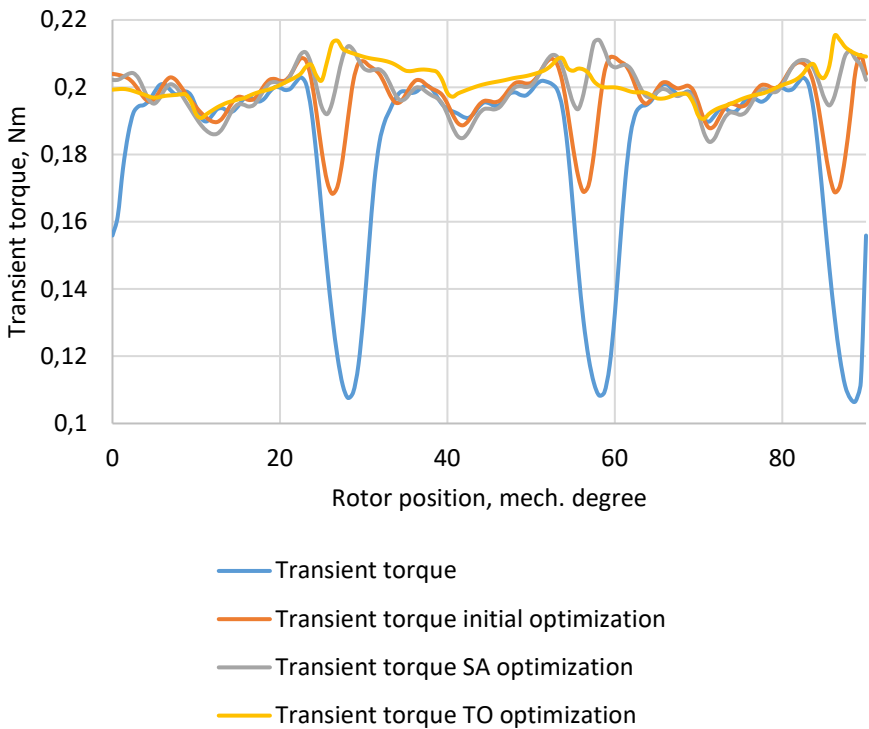
Figure 3-9: TO optimal design of SRM.



(a)



(b)



(c)

Figure 3-13: Comparison of the initial, initial optimal, SA optimal, and TO optimal designs of SRM in terms of: (a) real inductance profiles, (b) static phase torques, and (c) transient torque.

Table 3-7 summarizes in numbers all the results obtained during design, initial optimization, sensitivity analysis, and topology optimization. It can be obviously seen that the improvement of the SRM is significant. Compared to the initial design, the latest optimal solution helped to reduce the torque ripple by 77% while increasing the average torque by 10%.

Table 3-7: Optimization flow results.

Characteristic	Design			
	Initial	Initial optimal	Sensitivity analysis optimal	Topology optimization optimal
Average torque, Nm	0.181	0.197	0.199	0.201
Torque ripple	0.531	0.210	0.152	0.123

This section designed and optimized SRM. Additionally, this this section simulated the SRM, and explored various geometrical parameters and their effect on the average torque and torque ripple. Moreover, a novel optimization method was proposed which reduced the computational complexity of the TO. At first, the motor was designed using a classic design approach. Then, the main dimensions of the motor were optimized using the DOM along with the GA. A considerable improvement of the average torque and torque ripple were achieved. Particularly, the increase of the average torque 9% and reduction of torque ripple by 60% were noticed. Another step of the optimization was dedicated to the SA through which the average torque was upgraded by 10% and torque ripple condensed by 71% comparing to the initial design. As the last step, the TO cut out the torque ripple by 77%. It can be noticed that the main improvement of the torque quality was completed by the initial design optimization. Not surprisingly, the global parameters of the SRM geometry shape the performance the most. Such key dimensions as rotor diameters, stator and rotor poles angles have a huge impact on the SRM performance. Yet, through the application of the SA and usage of a new parameter such as the rotor pole angle at the core, additional 11% could be gained in the reduction of the torque ripple. Lastly, it can be seen that the TO optimization diminished the torque ripple by additional 6%. A potential of the TO could be open more in case of 3D TO and improvement of the additively manufactured motor characteristics considering inner structure of the motor and its influence not only on the torque ripple, but also on the core losses and thermal condition.

4 Conclusion

The purpose of the current thesis was to investigate the opportunities for SRM design, shape, and topology optimization. Moreover, this research was undertaken to explore the prospects that additive manufacturing provides for EMs optimization. Another aim of this study was to design and optimize a SRM, while presenting various methods of EMs optimization.

This thesis has reviewed extensive literature to show various optimization modeling techniques, methodologies, and algorithms. One of the most important conclusions of the introductory part of the thesis was a comprehensive comparison of various modeling techniques and methodologies in terms of accuracy, rapidity, simplicity, and flexibility. These conclusions provide insights into design optimization opportunities and open up the advantages and disadvantages of various optimization methodologies.

This research has also shown the opportunities opened up by rapidly developing additive manufacturing techniques. The possibilities of EMs additive manufacturing have been reviewed and presented in this thesis. This finding will be of interest to motor design and optimization researchers.

Another chapter of this thesis was dedicated to the design and optimization of the SRM with the aim to increase the average torque, decrease the core volume, and reduce the torque ripple. One of the most significant results of this study is the creation of a new multi-level optimization method. Initially, TO was selected as a promising approach toward SRM optimization. However, high computational complexity posed a challenge that could not be neglected. To overcome the issue of TO high time consumption, a novel method has been proposed. The proposed approach aimed to reduce the design space of the TO by applying initial optimization techniques and sensitivity analysis. The first step involved initial parameter optimization, where main geometrical parameters such as the diameters of the stator and rotor, pole angles, etc. were optimized using the direct optimization method. The result of this optimization was an optimized structure of the motor which could limit TO design space. Another step of the proposed approach was SA, which could identify the most vital areas of the SRM design for the average torque increase and reduction of the torque ripple. One of the most significant findings to emerge from the SA was limited design space that was taking less than 30% of the initial design space of the SRM. And final step of the optimization was TO in the selected area of the SRM. A significant increase in the average torque by 10% and a major reduction of the torque ripple by 70% were the results of the SRM optimization. This thesis has provided a deep insight into SRM optimization, covering in detail the design of the motor, selection, and setup of the optimization. These results add to the rapidly expanding field of EMs optimization and open up a new ground for SRM development.

5 Future studies

To benefit the highest performance of additively manufactured SRM, the 3D topology optimization (3D TO) should come into a greater focus. The 3D TO can open up a new ground of opportunities for the improvement of the SRM performance characteristics. It has been shown in this thesis, that 2D geometry of the SRM significantly influences the torque curve. On the other hand, recent literature presents the 3D modification possibilities such as rotor skewing for SRM torque ripple reduction. Another motor characteristic which could benefit from 3D TO is the thermal condition of the motor. Using 3D TO, novel heat transfer ways and geometries can be found. Last but not least, 3D TO can be of a good use for reducing the core losses of additively manufactured EM. A search for new lattice structures can be carried out by 3D TO. Taking into account the mentioned promising benefits of 3D TO, a further study should properly assess and carry out 3D TO.

More broadly, research into the control of SRM drive is also needed to fully alter the motor performance. It has been shown in this thesis, that control of SRM is very adaptive and flexible. Moreover, it has been observed, that the influence of the commutation parameters of the SRM control, visibly affects the torque of the motor. Therefore, commutation pattern parameters are suggested to be the elements of the future optimization.

References

- [1] P. Waide and C. U. Brunner, "Energy-Efficiency Policy Opportunities for Electric Motor-Driven Systems," *Int. energy agency*, vol. na, no. na, 2011.
- [2] C. U. Brunner, P. Waide, and M. Jakob, "Harmonized Standards for Motors and Systems Global progress report and outlook," 2011.
- [3] Y. Duan and D. M. Ionel, "A review of recent developments in electrical machine design optimization methods with a permanent magnet synchronous motor benchmark study," in *IEEE Energy Conversion Congress and Exposition: Energy Conversion Innovation for a Clean Energy Future, ECCE 2011, Proceedings*, 2011, pp. 3694–3701, doi: 10.1109/ECCE.2011.6064270.
- [4] S. Sato, T. Sato, and H. Igarashi, "Topology optimization of synchronous reluctance motor using normalized gaussian network," *IEEE Trans. Magn.*, vol. 51, no. 3, Mar. 2015, doi: 10.1109/TMAG.2014.2359679.
- [5] Maciej Serda *et al.*, "Manufacturing of topology optimized soft magnetic core through 3D printing," *Uniw. śląski*, vol. 7, no. 1, pp. 343–354, 2016, doi: 10.2/JQUERY.MIN.JS.
- [6] J. Dang, J. R. Mayor, S. A. Semidey, R. Harley, T. Habetler, and J. Restrepo, "Practical considerations for the design and construction of a high speed SRM with a flux-bridge rotor," in *2014 IEEE Energy Conversion Congress and Exposition, ECCE 2014*, Nov. 2014, pp. 3842–3849, doi: 10.1109/ECCE.2014.6953923.
- [7] W. Xu, J. Zhu, Y. Guo, S. Wang, Y. Wang, and Z. Shi, "Survey on electrical machines in electrical vehicles," *2009 Int. Conf. Appl. Supercond. Electromagn. Devices, ASEMD 2009*, no. c, pp. 167–170, 2009, doi: 10.1109/ASEMD.2009.5306667.
- [8] E. Andriushchenko *et al.*, "Sensitivity Analysis for Multi-Objective Optimization of Switched Reluctance Motors," *Mach. 2022, Vol. 10, Page 559*, vol. 10, no. 7, p. 559, Jul. 2022, doi: 10.3390/MACHINES10070559.
- [9] Y. Tang, G. Dong, Q. Zhou, and Y. F. Zhao, "Lattice Structure Design and Optimization with Additive Manufacturing Constraints," *IEEE Trans. Autom. Sci. Eng.*, vol. 15, no. 4, pp. 1546–1562, Oct. 2018, doi: 10.1109/TASE.2017.2685643.
- [10] E. Andriushchenko, M. H. Mohammadi, D. A. Lowther, H. Heidari, A. Kallaste, and A. Khan, "Topology Optimization of a 3D-Printed Switched Reluctance Motor," *2022 Int. Conf. Electr. Mach.*, pp. 1976–1980, Sep. 2022, doi: 10.1109/ICEM51905.2022.9910829.
- [11] G. Lei, J. Zhu, Y. Guo, C. Liu, and B. Ma, "A review of design optimization methods for electrical machines," *Energies*, vol. 10, no. 12, 2017, doi: 10.3390/en10121962.
- [12] H. Zhang and S. Wang, "Topology Optimization of Rotor Pole in Switched Reluctance Motor for Minimum Torque Ripple," <http://dx.doi.org/10.1080/15325008.2017.1310769>, vol. 45, no. 8, pp. 905–911, May 2017, doi: 10.1080/15325008.2017.1310769.
- [13] M. ROSU *et al.*, *MULTIPHYSICS SIMULATION BY DESIGN FOR ELECTRICAL MACHINES, POWER ELECTRONICS, AND DRIVES*. 2018.
- [14] J. M. Kokernak and D. A. Torrey, "Magnetic circuit model for the mutually coupled switched-reluctance machine," *IEEE Trans. Magn.*, vol. 36, no. 2, pp. 500–507, 2000, doi: 10.1109/20.825824.

- [15] W. Sun, Q. Li, L. Sun, L. Zhu, and L. Li, "Electromagnetic analysis on novel rotor-segmented axial-field srm based on dynamic magnetic equivalent circuit," *IEEE Trans. Magn.*, vol. 55, no. 6, Jun. 2019, doi: 10.1109/TMAG.2019.2901002.
- [16] N. Sadowski, "Finite elements coupled to electrical circuit equations in the simulation of switched reluctance drives: attention to mechanical behaviour," *IEEE Trans. Magn.*, vol. 32, no. 3 PART 2, pp. 1086–1089, 1996, doi: 10.1109/20.497430.
- [17] H. Chen, W. Yan, and Q. Wang, "Electromagnetic Analysis of Flux Characteristics of Double-Sided Switched Reluctance Linear Machine," *IEEE Trans. Appl. Supercond.*, vol. 26, no. 4, Jun. 2016, doi: 10.1109/TASC.2016.2539215.
- [18] H. Chen, X. Liu, and W. Yan, "Three-Dimensional Magnetic Equivalent Circuit Research of Double-Sided Switched Reluctance Linear Machine," *IEEE Trans. Appl. Supercond.*, vol. 30, no. 4, Jun. 2020, doi: 10.1109/TASC.2020.2990774.
- [19] S. H. Mao, D. Dorrell, and M. C. Tsai, "Fast analytical determination of aligned and unaligned flux linkage in switched reluctance motors based on a magnetic circuit model," *IEEE Trans. Magn.*, vol. 45, no. 7, pp. 2935–2942, Jul. 2009, doi: 10.1109/TMAG.2009.2016087.
- [20] D. Lin, P. Zhou, S. Stanton, and Z. J. Cendes, "An analytical circuit model of switched reluctance motors," *IEEE Trans. Magn.*, vol. 45, no. 12, pp. 5368–5375, Dec. 2009, doi: 10.1109/TMAG.2009.2024754.
- [21] D. S. Mihic, M. V. Terzic, and S. N. Vukosavic, "A New Nonlinear Analytical Model of the SRM with Included Multiphase Coupling," *IEEE Trans. Energy Convers.*, vol. 32, no. 4, pp. 1322–1334, Dec. 2017, doi: 10.1109/TEC.2017.2707587.
- [22] F. Soares and P. J. C. Branco, "Simulation of a 6/4 switched reluctance motor based on Matlab/Simulink environment," *IEEE Trans. Aerosp. Electron. Syst.*, vol. 37, no. 3, pp. 989–1009, Jul. 2001, doi: 10.1109/7.953252.
- [23] K. N. Srinivas and R. Arumugam, "Dynamic characterization of switched reluctance motor by computer-aided design and electromagnetic transient simulation," *IEEE Trans. Magn.*, vol. 39, no. 3 II, pp. 1806–1812, May 2003, doi: 10.1109/TMAG.2003.809839.
- [24] W. Lu, A. Keyhani, and A. Fardoun, "Neural network-based modeling and parameter identification of switched reluctance motors," *IEEE Trans. Energy Convers.*, vol. 18, no. 2, pp. 284–290, Jun. 2003, doi: 10.1109/TEC.2003.811738.
- [25] Y. Kano, T. Kosaka, and N. Matsui, "Magnetization characteristics analysis of SRM by simplified non-linear magnetic analysis," in *Proceedings of the Power Conversion Conference-Osaka 2002, PCC-Osaka 2002*, 2002, vol. 2, pp. 689–694, doi: 10.1109/PCC.2002.997602.
- [26] L. A. Belfore, "Modeling faulted switched reluctance motors using evolutionary neural networks," *IEEE Trans. Ind. Electron.*, vol. 44, no. 2, pp. 226–233, 1997, doi: 10.1109/41.564161.
- [27] T. Lachman, T. R. Mohamad, and C. H. Fong, "Nonlinear modelling of switched reluctance motors using artificial intelligence techniques," *IEE Proc. Electr. Power Appl.*, vol. 151, no. 1, pp. 53–60, Jan. 2004, doi: 10.1049/ip-epa:20040025.
- [28] H. P. Chi, R. L. Lin, and J. F. Chen, "Simplified flux-linkage model for switched-reluctance motors," in *IEE Proceedings: Electric Power Applications*, May 2005, vol. 152, no. 3, pp. 577–583, doi: 10.1049/ip-epa:20045207.
- [29] W. Ding and D. Liang, "A fast analytical model for an integrated switched reluctance starter/generator," *IEEE Trans. Energy Convers.*, vol. 25, no. 4, pp. 948–956, Dec. 2010, doi: 10.1109/TEC.2010.2052620.

- [30] A. Khalil and I. Husain, "A fourier series generalized geometry-based analytical model of switched reluctance machines," *IEEE Trans. Ind. Appl.*, vol. 43, no. 3, pp. 673–684, May 2007, doi: 10.1109/TIA.2007.895737.
- [31] X. Ding, M. Rashed, C. I. Hill, and S. Bozhko, "Analytical modelling approach for switched reluctance machines with deep saturation," Feb. 2017, doi: 10.1109/ESARS-ITEC.2016.7841411.
- [32] A. Radun, "Analytical calculation of the switched reluctance motor's unaligned inductance," *IEEE Trans. Magn.*, vol. 35, no. 6, pp. 4473–4481, 1999, doi: 10.1109/20.809140.
- [33] S. Li, S. Zhang, T. G. Habetler, and R. G. Harley, "Fast and accurate analytical calculation of the unsaturated phase inductance profile of 6/4 switched reluctance machines," 2016, doi: 10.1109/ECCE.2016.7855107.
- [34] Z. Djelloul-Khedda, K. Boughrara, F. Dubas, and R. Ibtouen, "Nonlinear Analytical Prediction of Magnetic Field and Electromagnetic Performances in Switched Reluctance Machines," *IEEE Trans. Magn.*, vol. 53, no. 7, Jul. 2017, doi: 10.1109/TMAG.2017.2679686.
- [35] J. Kumar, "Application of artificial neural networks to optimization problems in electrical power operation," 1993.
- [36] W. Ding and D. Liang, "Modeling of a 6/4 switched reluctance motor using adaptive neural fuzzy inference system," in *IEEE Transactions on Magnetics*, Jul. 2008, vol. 44, no. 7, pp. 1796–1804, doi: 10.1109/TMAG.2008.919711.
- [37] Z. Lin, D. S. Reay, B. W. Williams, and X. He, "Online modeling for switched reluctance motors using b-spline neural networks," *IEEE Trans. Ind. Electron.*, vol. 54, no. 6, pp. 3317–3322, Dec. 2007, doi: 10.1109/TIE.2007.904009.
- [38] S. Song, M. Zhang, and L. Ge, "A new decoupled analytical modeling method for switched reluctance machine," *IEEE Trans. Magn.*, vol. 51, no. 3, Mar. 2015, doi: 10.1109/TMAG.2014.2363214.
- [39] L. Shen, J. Wu, S. Yang, and X. Huang, "Fast flux linkage measurement for switched reluctance motors excluding rotor clamping devices and position sensors," *IEEE Trans. Instrum. Meas.*, vol. 62, no. 1, pp. 185–191, 2013, doi: 10.1109/TIM.2012.2212598.
- [40] X. Cui, J. Sun, C. Gan, C. Gu, and Z. Zhang, "Optimal design of saturated switched reluctance machine for low speed electric vehicles by subset quasi-orthogonal algorithm," *IEEE Access*, vol. 7, pp. 101086–101095, 2019, doi: 10.1109/ACCESS.2019.2929103.
- [41] K. Diao, X. Sun, G. Lei, Y. Guo, and J. Zhu, "Multiobjective system level optimization method for switched reluctance motor drive systems using finite-element model," *IEEE Trans. Ind. Electron.*, vol. 67, no. 12, pp. 10055–10064, Dec. 2020, doi: 10.1109/TIE.2019.2962483.
- [42] J. W. Lee, H. S. Kim, B. Il Kwon, and B. T. Kim, "New rotor shape design for minimum torque ripple of SRM using FEM," in *IEEE Transactions on Magnetics*, Mar. 2004, vol. 40, no. 2 II, pp. 754–757, doi: 10.1109/TMAG.2004.824803.
- [43] K. Kiyota, T. Kakishima, H. Sugimoto, and A. Chiba, "Comparison of the test result and 3D-FEM analysis at the knee point of a 60 kW SRM for a HEV," *IEEE Trans. Magn.*, vol. 49, no. 5, pp. 2291–2294, 2013, doi: 10.1109/TMAG.2013.2242453.
- [44] M. Abbasian, M. Moallem, and B. Fahimi, "Double-stator switched reluctance machines (DSSRM): Fundamentals and magnetic force analysis," *IEEE Trans. Energy Convers.*, vol. 25, no. 3, pp. 589–597, Sep. 2010, doi: 10.1109/TEC.2010.2051547.

- [45] T. F. Chan, W. Wang, and L. L. Lai, "Performance of an axial-flux permanent magnet synchronous generator from 3-D finite-element analysis," *IEEE Trans. Energy Convers.*, vol. 25, no. 3, pp. 669–676, Sep. 2010, doi: 10.1109/TEC.2010.2042057.
- [46] C. Lu, P. Zhou, D. Lin, B. He, and D. Sun, "Multiply connected 3-D transient problem with rigid motion associated with mbi T-mmb Ω formulation," *IEEE Trans. Magn.*, vol. 50, no. 2, pp. 449–452, 2014, doi: 10.1109/TMAG.2013.2280875.
- [47] P. Zhou, Z. Badics, D. Lin, and Z. J. Cendes, "Nonlinear T- Ω formulation including motion for multiply connected 3-D problems," *IEEE Trans. Magn.*, vol. 44, no. 6, pp. 718–721, Jun. 2008, doi: 10.1109/TMAG.2007.915118.
- [48] D. Lin, P. Zhou, Q. M. Chen, N. Lambert, and Z. J. Cendes, "The effects of steel lamination core losses on 3d transient magnetic fields," in *IEEE Transactions on Magnetism*, Aug. 2010, vol. 46, no. 8, pp. 3539–3542, doi: 10.1109/TMAG.2010.2043509.
- [49] W. Yao, J. M. Jin, and P. T. Krein, "A highly efficient domain decomposition method applied to 3-D finite-element analysis of electromechanical and electric machine problems," *IEEE Trans. Energy Convers.*, vol. 27, no. 4, pp. 1078–1086, 2012, doi: 10.1109/TEC.2012.2216528.
- [50] P. Zhou, B. He, C. Lu, D. Lin, and N. Chen, "Transient simulation of electrical machines using time decomposition method," Aug. 2017, doi: 10.1109/IEMDC.2017.8002034.
- [51] H. Chen, W. Yan, J. J. Gu, and M. Sun, "Multiobjective Optimization Design of a Switched Reluctance Motor for Low-Speed Electric Vehicles with a Taguchi-CSO Algorithm," *IEEE/ASME Trans. Mechatronics*, vol. 23, no. 4, pp. 1762–1774, Aug. 2018, doi: 10.1109/TMECH.2018.2839619.
- [52] B. Anvari, H. A. Toliyat, and B. Fahimi, "Simultaneous Optimization of Geometry and Firing Angles for In-Wheel Switched Reluctance Motor Drive," *IEEE Trans. Transp. Electrification*, vol. 4, no. 1, pp. 322–329, 2017, doi: 10.1109/TTE.2017.2766452.
- [53] W. Tong, *Mechanical design of electric motors*. 2014.
- [54] H. Y. Yang, Y. C. Lim, and H. C. Kim, "Acoustic noise/vibration reduction of a single-phase SRM using skewed stator and rotor," *IEEE Trans. Ind. Electron.*, vol. 60, no. 10, pp. 4292–4300, 2013, doi: 10.1109/TIE.2012.2217715.
- [55] K. N. Srinivas and R. Arumugam, "Analysis and characterization of Switched reluctance motors: Part II - Flow, thermal, and vibration analyses," *IEEE Trans. Magn.*, vol. 41, no. 4, pp. 1321–1332, Apr. 2005, doi: 10.1109/TMAG.2004.843349.
- [56] K. N. Srinivas and R. Arumugam, "Static and dynamic vibration analyses of switched reluctance motors including bearings, housing, rotor dynamics, and applied loads," *IEEE Trans. Magn.*, vol. 40, no. 4 I, pp. 1911–1919, Jul. 2004, doi: 10.1109/TMAG.2004.828034.
- [57] M. Takiguchi, H. Sugimoto, N. Kurihara, and A. Chiba, "Acoustic Noise and Vibration Reduction of SRM by Elimination of Third Harmonic Component in Sum of Radial Forces," *IEEE Trans. Energy Convers.*, vol. 30, no. 3, pp. 883–891, Sep. 2015, doi: 10.1109/TEC.2015.2401398.
- [58] J. W. Ahn, S. J. Park, and D. H. Lee, "Hybrid excitation of SRM for reduction of vibration and acoustic noise," *IEEE Trans. Ind. Electron.*, vol. 51, no. 2, pp. 374–380, Apr. 2004, doi: 10.1109/TIE.2004.825227.

- [59] W. Yan *et al.*, “Design and multi-objective optimisation of switched reluctance machine with iron loss,” *IET Electr. Power Appl.*, vol. 13, no. 4, pp. 435–444, Apr. 2019, doi: 10.1049/iet-epa.2018.5699.
- [60] W. Wu, J. B. Dunlop, S. J. Collocott, and B. A. Kalan, “Design Optimization of a Switched Reluctance Motor by Electromagnetic and Thermal Finite-Element Analysis,” in *IEEE Transactions on Magnetics*, Sep. 2003, vol. 39, no. 5 II, pp. 3334–3336, doi: 10.1109/TMAG.2003.816248.
- [61] Y. Huang, J. Zhu, and Y. Guo, “Thermal analysis of high-speed SMC motor based on thermal network and 3-D FEA with rotational core loss included,” in *IEEE Transactions on Magnetics*, Oct. 2009, vol. 45, no. 10, pp. 4680–4683, doi: 10.1109/TMAG.2009.2023065.
- [62] S. Nategh, O. Wallmark, M. Leksell, and S. Zhao, “Thermal analysis of a PMA SRM using partial FEA and lumped parameter modeling,” *IEEE Trans. Energy Convers.*, vol. 27, no. 2, pp. 477–488, 2012, doi: 10.1109/TEC.2012.2188295.
- [63] E. Andriushchenko *et al.*, “Optimization of a 3D-Printed Permanent Magnet Coupling Using Genetic Algorithm and Taguchi Method,” *Electronics*, vol. 10, no. 4, p. 494, Feb. 2021, doi: 10.3390/electronics10040494.
- [64] A. A. Arkadan, M. N. Elbsat, and M. A. Mneimneh, “Particle swarm design optimization of a rotor Synrm for traction applications,” *IEEE Trans. Magn.*, vol. 45, no. 3, pp. 956–959, Mar. 2009, doi: 10.1109/TMAG.2009.2012482.
- [65] J. Y. Lee, J. H. Chang, D. H. Kang, S. Il Kim, and J. P. Hong, “Tooth shape optimization for cogging torque reduction of transverse flux rotary motor using design of experiment and response surface methodology,” in *IEEE Transactions on Magnetics*, Apr. 2007, vol. 43, no. 4, pp. 1817–1820, doi: 10.1109/TMAG.2007.892611.
- [66] K. Diao, X. Sun, G. Lei, G. Bramerdorfer, Y. Guo, and J. Zhu, “Robust Design Optimization of Switched Reluctance Motor Drive Systems Based on System-Level Sequential Taguchi Method,” *IEEE Trans. Energy Convers.*, vol. 36, no. 4, pp. 3199–3207, 2021, doi: 10.1109/TEC.2021.3085668.
- [67] L. Gargalis *et al.*, “Additive Manufacturing and Testing of a Soft Magnetic Rotor for a Switched Reluctance Motor,” *IEEE Access*, p. 1, 2020, doi: 10.1109/ACCESS.2020.3037190.
- [68] H. Tiismus, *Production and Properties of Additively Manufactured Electrical Machine Cores*. .
- [69] A. Kallaste, T. Vaimann, and A. Rassõlkin, “Additive Design Possibilities of Electrical Machines,” in *2018 IEEE 59th International Scientific Conference on Power and Electrical Engineering of Riga Technical University (RTU CON)*, 2018, pp. 1–5, doi: 10.1109/RTU CON.2018.8659828.
- [70] H. Tiismus, A. Kallaste, T. Vaimann, and A. Rassõlkin, “Eddy Current Loss Reduction Prospects in Laser Additively Manufactured Soft Magnetic Cores,” *2022 Int. Conf. Electr. Mach.*, pp. 1511–1516, Sep. 2022, doi: 10.1109/ICEM51905.2022.9910679.
- [71] B. Khoshoo, K. J. Islam, H. Suen, P. Kwon, J. P. Lozano, and S. N. Foster, “Eddy Current Loss Reduction in Binder Jet Printed Iron Silicon Cores,” *2022 Int. Conf. Electr. Mach.*, pp. 558–564, Sep. 2022, doi: 10.1109/ICEM51905.2022.9910749.
- [72] A. Credo, E. Kurvinen, I. Petrov, and J. Pyrhonen, “Investigation of Material Combinations for Axially-Laminated Synchronous Machine,” *2022 Int. Conf. Electr. Mach.*, pp. 814–820, Sep. 2022, doi: 10.1109/ICEM51905.2022.9910821.

- [73] R. Notari, M. Pastura, S. Nuzzo, D. Barater, G. Franceschini, and C. Gerada, "AC losses reduction in Hairpin Windings produced via Additive Manufacturing," *2022 Int. Conf. Electr. Mach.*, pp. 1144–1149, Sep. 2022, doi: 10.1109/ICEM51905.2022.9910620.
- [74] "Siemens. Simcenter MAGNET 2D/3D, 2021. [Online]." <https://www.plm.automation.siemens.com/global/en/products/simcenter/magnet.html> (accessed Jun. 28, 2021).
- [75] E. Andriushchenko, J. Kaska, A. Kallaste, A. Belahcen, T. Vaimann, and A. Rassõlkin, "Design Optimization of Permanent Magnet Clutch with Ārtap Framework," *Period. Polytech. Electr. Eng. Comput. Sci. Des. Optim. Perm. Magn. Clutch with Ārtap Framew. Period. Polytech. Electr. Eng. Comput. Sci. (in Press.*
- [76] K. C. Yong, S. Y. Hee, and S. K. Chang, "Pole-shape optimization of a switched-reluctance motor for torque ripple reduction," *IEEE Trans. Magn.*, vol. 43, no. 4, pp. 1797–1800, 2007, doi: 10.1109/TMAG.2006.892292.
- [77] C. Midha, "A Study of Topology Optimization Methods for the Design of Electromagnetic Devices," 2018.
- [78] Y. Hidaka and H. Igarashi, "Topology Optimization of Synchronous Reluctance Motors Considering Localized Magnetic Degradation Caused by Punching," *IEEE Trans. Magn.*, vol. 53, no. 6, Jun. 2017, doi: 10.1109/TMAG.2017.2659721.

Acknowledgements

My sincere gratitude to my supervisors for their continuous support and guidance. I am thankful for help and support that I received from my family along all the way of my PhD study.

This work was supported by the Estonian Research Council with the grant PRG 1827 Additive Manufacturing of Electrical Machines.

Abstract

Design Optimization Methods of Additively Manufactured Switched Reluctance Motor

This Ph.D. dissertation presents switched reluctance motor (SRM) design and optimization. The study focused on the improvement of SRM torque characteristics using topology optimization (TO). In parallel, the TO challenge such as computational complexity was addressed.

Thanks to the rapid growth of advanced power electronics, SRMs have received a close attention from research and industry. Due to their simple and rigid structure, they are now considered as promising motors for various applications. However, SRMs' torque ripple presence slows down their development. Therefore, this thesis was motivated to apply powerful optimization techniques to improve SRM torque characteristics. The aim of this thesis was to optimize design of a SRM in order to increase the average torque, reduce the volume of the core material, and shrink the torque ripple. Additionally, additive manufacturing (AM) was proposed as a capable method of optimal designs production. AM was shown as strong support of motor optimization, thanks to the vast design opportunities that AM provides for motor manufacturing, optimization can be carried out at a more delicate level.

This work started with the review and assessment of the optimization environment elements such as models, methods, and algorithms. The SRMs modelling methods were scrutinized and the superiorities and the drawbacks of them were recognised. Different motor modelling approaches were studied and compared concerning their efficiency. Key optimization methods, models, and algorithms were researched. A comprehensive comparison of various optimization environments was carried out. Moreover, a procedure of the optimization environment section was created baring in mind accuracy of optimization results, computational complexity of the optimization, and manufacturability of optimised motor.

TO was selected as a promising optimization method for SRM's torque quality improvement. To overcome computational burden that TO imposes, a novel optimization approach is proposed in this thesis. The proposed method was a multi-level optimization method and included pre-optimization that could reduce the design space of the TO and consequently, decrease the TO computational complexity. Firstly, design optimization was carried out to increase the average torque of the SRM and reduce the volume of the core material. As a result, the torque characteristic of the motor was improved and the geometry focus shifted on the rotor and stator teeth. Then, a sensitivity analysis (SA) of unique design parameters of the SRM was carried out. The SA provided valuable information regarding the influence of the advance shapes of the rotor and stator teeth on the average torque and torque ripple. The design optimization and SA could help the TO focus on the very important areas of the motor and reduced the TO design space by more than 70%.

The resulting improvement of the SRM torque was significant. Thanks to the proposed approach, the average torque of the motor was increased by 10% while the torque ripple was reduced by 77%. At last, the initial and optimal designs of the SRM were manufactured using AM techniques.

Lühikokkuvõte

Kihtlisandustehnoloogia abil toodetud samm-mootori optimeerimise meetodid

Käesolev doktoritöö käsitleb endas samm-mootori (SRM) projekteerimist ja optimeerimist. Uuringus keskenduti SRM-i pöördemomendi omaduste parandamisele, kasutades topoloogia optimeerimist (TO). Paralleelselt käsitleti ka topoloogia optimeerimisega kaasnevaid probleeme, nagu arvutuslik keerukus.

Tänu jõuelektroonika kiirele arengule on kasvanud ka teadlaste ja tööstuse suur huvi SRMide vastu. Tänu nende lihtsale ja jäigale struktuurile peetakse neid nüüd paljulubavateks mootoriteks erinevate rakenduste jaoks. Samas üheks probleemiks on pöördemomendi pulsatsioon SRMidel, mis piirab nende arengut. Seetõttu võetigi lõputöö eesmärgiks SRM-i pöördemomendi omaduste parandamine kasutades selleks kaasaegseid optimeerimistehnikaid. Lõputöös käsitletaksegi SRM-i konstruktsiooni optimeerimist eesmärgiga suurendada keskmist pöördemomenti, vähendada magnetsüdamik materjali kulu ning vähendada pöördemomendi pulsatsiooni. Kuna optimaalset disainilahendust on keerukas toota traditsiooniliste meetoditega, siis töös pakuti välja ka masina tootmine kihtlisandustehnoloogia (AM) abil. AM on mootori optimeerimisel tugevaks toeks, tänu ulatuslikele disainivõimalustele, mida AM pakub mootori valmistamiseks, kuna optimeerimist saab teostada keerukamal tasemel.

Esmalt teostati töös optimeerimiskeskonna elementide, nagu mudelid, meetodid ja algoritmid, ülevaatamine ja hindamine. Uuriti SRM-i modelleerimismeetodeid ning tuvastati nende eelised ja puudused. Uuriti ja võrreldi erinevaid mootorite modelleerimise lähenemisviise lähtudes nende keerukusest. Viidi läbi sobivate optimeerimismeetodite, mudelite ja algoritmide analüüs, ning teostati erinevate optimeerimiskeskondade põhjalik võrdlus. Lisaks töötati välja protseduur optimeerimiskeskonna jaoks, mis võtaks arvesse optimeerimistulemuste täpsust, optimeerimise arvutuslikku keerukust ja optimeeritud mootori valmistatavust.

SRM-i pöördemomendi kvaliteedi parandamiseks leiti sobivaimaks optimeerimismetoodikaks TO. Töös pakutakse välja uudne optimeerimismetoodika, mis lihtsustaks TO-st tulenevat arvutusliku koormust. Väljapakutud meetodika on mitmetasandiline optimeerimismeetod sisaldades endas eeloptimeerimist, mis vähendab TO projekteerimisruumi ja läbi selle vähendab TO arvutuslikku keerukust. Esmalt teostati disaini optimeerimine, suurendamaks SRM-i keskmist pöördemomenti ja vähendades südamik materjali mahtu. Selle tulemusena paranevad mootori pöördemomendi omadused ning geomeetria fookus nihkub rootori ja staatori hammastele. Seejärel teostatakse SRM-i ainulaadsete konstruktsiooniparameetrite tundlikkuse analüüs (SA). Analüüs annab väärtuslikku teavet rootori ja staatori hammaste kuju mõju kohta keskmisele pöördemomendile ja pöördemomendi pulsatsioonile. Projekteerimise optimeerimine ja SA aitavad TO-l keskenduda mootori väga olulistele piirkondadele ja vähendavad TO projekteerimisruumi mahtu rohkem kui 70% võrra.

Töö tulemuseks on SRM-i pöördemomendi märkimisväärne paranemine. Tänu kavandatud lähenemisviisile suudeti suurendada mootori keskmist pöördemomenti 10% võrra, samas kui pöördemomendi pulsatsioon vähenes 77%. Valmistati ka SRM-i esialgne ja optimaalne prototüüp AM-tehnika abil.

Appendix

Publication I

Andriushchenko E., Mohammadi M. H., Lowther D. A., Heidari H., Kallaste. A. (2022). Topology optimization of a 3D-printed switched reluctance motor. 2022 International Conference on Electrical Machines (ICEM), Valencia, Spain, pp. 1976–1980, 2022.

Publication II

Andriushchenko E., Kallaste A., Mohammadi M. H., Lowther D. A., Heidari H. (2022). Sensitivity analysis for multi-objective optimization of switched reluctance motors. *MDPI Machines* 10(7), 559.

Publication IV

Andriushchenko E., Kaska J., Kallaste A., Belahcen A., Vaimann T., Rassolkin A. (2021). Design optimization of a permanent magnet clutch with Artap framework. *Periodica Polytechnica Electrical Engineering and Computer Science*, 65(2), pp. 106–112, 2021.

Publication V

Andriushchenko E., Kallaste A., Heidari H., Belahcen A., Vaimann T., Rassolkin A. (2020). Design optimization of permanent magnet clutch. 2020 International Conference on Electrical Machines (ICEM), pp. 436–440, 2020.

Curriculum vitae

Personal data

Name:	Ekaterina Andriushchenko
Date of birth:	15/01/1996
Place of birth:	Russia
Citizenship:	Russian

Contact data

E-mail:	katarina.and96@gmail.com
---------	--------------------------

Education

2019–now	PhD, Tallinn University of Technology (Electrical Power Engineering and Mechatronics)
2017–2019	MSC, at Peter the Great St. Petersburg Polytechnic University (Institute of Machinery, Materials, and Transport)
2013–2017	BSC, at Peter the Great St. Petersburg Polytechnic University (Institute of Machinery, Materials, and Transport)

Language competence

English	Fluent
Russian	Native
German	Intermediate

Elulookirjeldus

Isikuandmed

Nimi: Ekaterina Andriushchenko
Sünniaeg: 15/01/1996
Sünnikoht: Venemaa
Kodakondsus: Vene

Kontaktandmed

E-post: katarina.and96@gmail.com

Hariduskäik

2019–... PhD, Tallinna Tehnikaülikool (Elektroenergeetika ja mehhatroonika)
2017–2019 MSC, Peeter suure nimeline polütehniline ülikool (Masinate, materjalide ja transpordi instituut)
2013–2017 BSC, Peeter suure nimeline polütehniline ülikool (Masinate, materjalide ja transpordi instituut)

Keelteoskus

Vene keel Emakeel
Inglise keel Kõrgtase
Saksakeel Algtase